

Sulfur Transfer Reactions of a Zinc Tetrasulfanido Complex

Moises Ballesteros II and Emily Y. Tsui*

Department of Chemistry and Biochemistry, University of Notre Dame, Notre Dame, Indiana
46556, United States

Table of Contents

<i>Experimental Section</i>	S3
General Considerations	S3
Synthetic Procedures	S4
Scheme S1. Synthesis of [Et ₄ N] ₂ [LOMeZn].	S4
Characterization	S7
Figure S1. ¹ H NMR spectrum of dimethyl 4-methoxypyridine-2,6-dicarboxylate in CDCl ₃ at 25 °C.	S7
Figure S2. ¹ H NMR spectrum of 4-methoxypyridine-2,6-dicarboxylic acid in <i>d</i> ₆ -DMSO at 25 °C.	S8
Figure S3. ¹ H NMR spectrum of 4-methoxypyridine-2,6-dicarbonyl chloride in C ₆ D ₆ at 25 °C.	S8
Figure S4. ¹ H NMR spectrum of S1 in CDCl ₃ at 25 °C.	S9
Figure S5. ¹ H NMR spectrum of H ₄ LOMe in CDCl ₃ at 25 °C.	S9
Figure S6. ¹ H NMR spectrum of [Et ₄ N] ₂ [LOMeZn] in <i>d</i> ₆ -DMSO at 25 °C.	S10
Figure S7. ¹³ C NMR spectrum of [Et ₄ N] ₂ [LOMeZn] in <i>d</i> ₆ -DMSO at 25 °C.	S10
Figure S8. ¹ H NMR spectrum of [Et ₄ N] ₂ [2] in <i>d</i> ₆ -DMSO at 25 °C.	S11
Figure S9. ¹³ C NMR spectrum of [Et ₄ N] ₂ [2] in <i>d</i> ₆ -DMSO at 25 °C.	S11
Figure S10. ¹ H NMR spectrum of [Et ₄ N] ₂ [3] in <i>d</i> ₆ -DMSO at 25 °C.	S12
Figure S11. ¹³ C NMR spectrum of [Et ₄ N] ₂ [3] in <i>d</i> ₆ -DMSO at 25 °C.	S12
Figure S12. ¹ H NMR spectrum of H ₂ LS ³ in CDCl ₃ at 25 °C.	S13
Figure S13. UV-Vis spectrum of [Et ₄ N] ₂ [1] in CH ₃ CN.	S13
Figure S14. UV-Vis spectrum of [Et ₄ N] ₂ [2] in CH ₃ CN.	S14
Reactions	S15
Figure S15. ¹ H NMR spectra of [Et ₄ N] ₂ [1], a 1:1 mixture of [Et ₄ N] ₂ [1], and [Et ₄ N] ₂ [LOMeZn], [Et ₄ N] ₂ [LOMeZn], and [Et ₄ N] ₂ [LZn] in <i>d</i> ₆ -DMSO at 25 °C.	S15
Figure S16. ¹ H NMR spectra of a mixture of (TMEDA)ZnS ₆ and [Et ₄ N] ₂ [LZn] in <i>d</i> ₆ -DMSO, [Et ₄ N] ₂ [LZn] in <i>d</i> ₆ -DMSO, and (TMEDA)ZnS ₆ in <i>d</i> ₅ -pyridine at 25 °C.	S16
Figure S17. ¹ H NMR spectra of [Et ₄ N] ₂ [(L ^{Me} Zn) ₂] and a mixture of [Et ₄ N] ₂ [1] and methyl iodide (1.1 equiv) in <i>d</i> ₆ -DMSO at 25 °C.	S17
Figure S18. ¹ H NMR spectrum of L ^{Me2} Zn and a mixture of [Et ₄ N] ₂ [1] and methyl	S18

iodide (2.2 equiv) in *d*₆-DMSO at 25 °C.

Figure S19. ¹H NMR spectrum of a mixture of **A** and methyl iodide (1.8 equiv) in *d*₆-DMSO at 25 °C. S19

Figure S20. ¹H NMR spectra of oxidized H₄L and the organic product obtained after treatment of **A** with water in CDCl₃ at 25 °C. S20

Scheme S2. Representation of the possible products obtained via scrambling of tetrasulfanido moiety with ³⁴S. S21

Figure S21. EI mass spectrum of natural abundance sulfur in CH₃CN. The lowest *m/z* values correspond to S₂⁺ ions. S21

Figure S22. EI mass spectrum of natural abundance sulfur in CH₃CN. The picked *m/z* peaks correspond to S₄⁺-S₆⁺ ions. S22

Figure S23. EI mass spectrum of ³⁴S₈ in CH₃CN. The lowest *m/z* values correspond to S₂⁺ ions. S22

Figure S24. EI mass spectrum of ³⁴S₈ in CH₃CN. The picked *m/z* peaks correspond to S₄⁺-S₆⁺, and S₈⁺ ions. S23

Figure S25. EI mass spectrum of combined natural abundance S₈ and ³⁴S₈ in CH₃CN. The lowest *m/z* values correspond to S₂⁺ ions. S23

Figure S26. EI mass spectrum of combined natural abundance S₈ and ³⁴S₈ in CH₃CN. The picked *m/z* peaks correspond to S₄⁺-S₆⁺, and S₈⁺ ions. S24

Figure S27. Electronic absorption spectra of a mixture of [Et₄N]₂[**1**] and DMAD (1 equiv) at 5.0 × 10⁻⁴ M in CH₃CN. S26

Figure S28. Electronic absorption spectra of a mixture of [Et₄N]₂[**1**] and DMAD (10 equiv) at 2.5 × 10⁻⁴ M in CH₃CN. S26

Figure S29. Electronic absorption spectra of **A**, [**2**]²⁻, and [**3**]²⁻ S27

Figure S30. Concentrations of **A**, [**2**]²⁻, and [**3**]²⁻ plotted over time. S27

Crystallographic Information S28

Table S1. Crystal and refinement data. S28

References S30

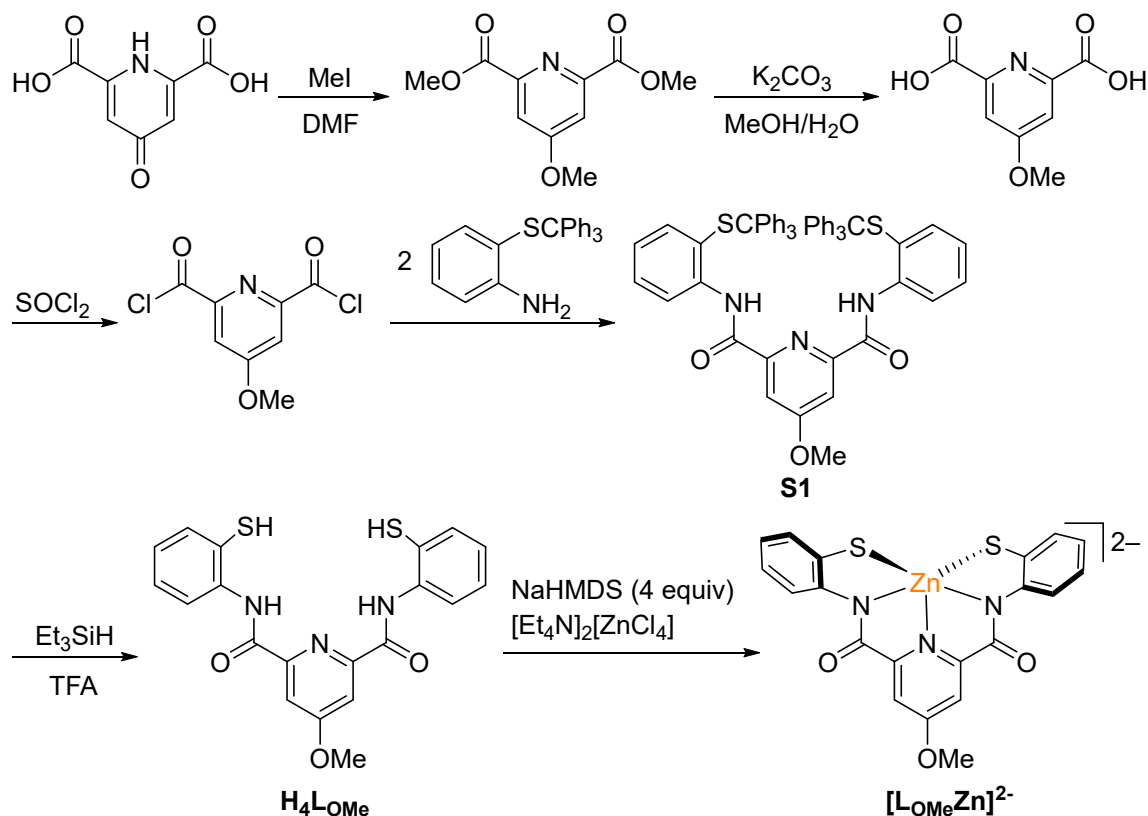
Experimental Section

General Considerations. Unless indicated otherwise, reactions were carried out in oven-dried glassware in a MBraun glovebox under an atmosphere of purified nitrogen. Anhydrous diethyl ether, THF, toluene, hexanes, and CH₃CN were dried using the Grubbs method on a J.C. Meyer solvent system.¹ *N,N*-dimethylformamide (DMF) and triethylamine were dried by refluxing over CaH₂ under nitrogen, then distilled under vacuum. Acetone was vacuum transferred from CaSO₄ twice, degassed under vacuum in a dry-ice/acetone bath, and stored under nitrogen. Dimethyl sulfoxide (DMSO) was degassed under vacuum then filtered three times through plugs of activated alumina under nitrogen, and stored over activated molecular sieves (4Å). *d*₆-DMSO was purchased from Cambridge Isotope Laboratories and distilled twice from molecular sieves (4Å). *d*₃-Acetonitrile (CD₃CN) was purchased from Cambridge Isotope Laboratories, dried over CaH₂, and vacuum transferred. Celite was dried under vacuum at 300 °C for 3 days. ¹H and ¹³C NMR spectra were recorded on a Bruker 400 MHz instrument or a Bruker 500 MHz instrument with shifts reported relative to the residual solvent peak (¹H, δ = 2.50 ppm and ¹³C, δ = 39.5 ppm for *d*₆-DMSO. ¹H, δ = 1.94 ppm and ¹³C, δ = 1.32 ppm, 118.26 ppm for *d*₃-CD₃CN. ¹H, δ = 7.27 ppm and ¹³C, δ = 77.16 ppm for CDCl₃. ¹H, δ = 7.16 ppm and ¹³C, δ = 128.06 ppm for C₆D₆).

Electrospray ionization mass spectroscopy (ESI-MS) and electron ionization mass spectroscopy (EI-MS) were performed at the University of Notre Dame Mass Spectrometry & Proteomics Facility on a Bruker microTOF-Q II instrument and a Waters GCT Premiere instrument, respectively. Elemental analysis was performed by Midwest Microlabs, LLC, Indianapolis, IN. Electronic absorption spectra were taken on an Agilent Cary 60 spectrophotometer.

Unless otherwise indicated, all commercial chemicals were used without further purification. Sulfur (S₈) was purchased from Beantown Chemicals and was recrystallized from hot toluene and stored under nitrogen. ³⁴S₈ was purchased from Icon Isotopes. Dimethyl acetylenedicarboxylate (DMAD) was purchased from Aldrich, distilled under vacuum, and stored under nitrogen. Sulfur dichloride (SCl₂) was purchased from Aldrich, distilled under nitrogen, and stored in the dark under nitrogen. Methyl iodide (MeI) was purchased from Aldrich and used without further purification. ZnCl₂ was purchased from Strem. Sodium bis(trimethylsilyl)amide (NaHMDS) and trimethoxybenzene were purchased from Acros. Thionyl chloride (SOCl₂) was purchased from TCI. Trifluoroacetic acid (TFA) and triethylsilane (Et₃SiH) were purchased from Oakwood. Chelidamic acid was purchased from Matrix Scientific. The synthesis of [LZn]²⁻ and [1]²⁻ have been previously described.² (TMEDA)ZnS₆ was synthesized according to literature procedures.³

Synthetic Procedures



Scheme S1. Synthesis of methoxy-substituted zinc dithiolate complex, [L_{OMe}Zn]²⁻.

Synthesis of dimethyl 4-methoxypyridine-2,6-dicarboxylate.⁴ A flame-dried Schlenk flask equipped with a stir bar was charged with dry DMF (15 mL), chelidamic acid (1.00 g, 5.46 mmol, 1 equiv), and K₂CO₃ (4.00 g, 28.9 mmol, 5.3 equiv). The brown mixture was stirred at 40 °C under N₂ for 24 h. The resulting mixture was cooled to room temperature, filtered through Celite, and washed with CH₂Cl₂. The solution was washed with brine, dried over MgSO₄, filtered, and dried under vacuum to yield a brown residue. This product was carried on without further purification. ¹H NMR (CDCl₃, 400 MHz): δ 7.82 (s, 2 H), 4.02 (s, 6 H), 3.99 (s, 3 H) ppm.

Synthesis of 4-methoxypyridine-2,6-dicarboxylic acid.⁵ The dimethyl 4-methoxypyridine-2,6-dicarboxylate prepared in the previous step was taken up in a mixture of 2:1 MeOH/H₂O (45 mL). K₂CO₃ (5.00 g, 35.2 mmol) was added, and the mixture was stirred for 12 h at room temperature. The resulting mixture was poured over ice/conc. HCl (5 mL), then dried under vacuum to yield a mixture of the product and KCl as a brown solid. This mixture was carried on without further purification. ¹H NMR (*d*₆-DMSO, 400 MHz): δ 7.72 (s, 2 H), 3.96 (s, 3 H) ppm.

Synthesis of 4-methoxypyridine-2,6-dicarbonyl chloride (S1).⁵ A 100-mL round-bottom flask equipped with a stir bar was charged with the unpurified 4-methoxypyridine-2,6-dicarboxylic acid prepared in the previous step and SOCl₂ (15.0 mL, 207 mmol, 37.9 equiv). The mixture was

refluxed under N₂ for 48 h, then cooled to room temperature. Excess SOCl₂ was distilled off under nitrogen, and the resulting brown residue was dried under vacuum. In the glovebox, the brown solid was taken up in THF (20 mL) and filtered through Celite to remove KCl. The filtrate was concentrated *in vacuo* to yield the product as a brown solid that was carried forward without further purification (0.730 g, 57% over 3 steps). ¹H NMR (C₆D₆, 400 MHz): δ 7.03 (s, 2 H), 2.70 (s, 3 H) ppm.

Synthesis of triphenylmethyl bis(2'-sulfidophenyl)-4-methoxypyridine-2,6-dicarboxamide (S1). In the glovebox, an oven-dried 250-mL three-necked round-bottom flask equipped with a stir bar was charged with 4-methoxypyridine-2,6-dicarbonyl chloride (0.730 g, 3.13 mmol, 1 equiv) and dry CH₂Cl₂ (20 mL). Triethylamine (3.0 mL, 22 mmol, 7.0 equiv) was added, followed by a solution of triphenylmethyl 2-sulfidoaniline (2.36 g, 6.42 mmol, 2.05 equiv) in CH₂Cl₂ (30 mL). The flask was fit with a nitrogen inlet adapter, then stirred under N₂ at room temperature for 15 h. The resulting solution was washed with brine twice, dried over MgSO₄, filtered, and dried *in vacuo* to yield a brown solid. This residue was recrystallized from hot hexanes/CH₂Cl₂ to yield the product as an off-white solid (1.4 g, 50%). ¹H NMR (CDCl₃, 400 MHz): δ 10.68 (s, 2 H, NH), 8.63 (d, *J* = 8.7 Hz, 2 H), 7.71 (s, 2 H), 7.52 (m, 4 H), 7.11 (d, *J* = 7.4 Hz, 12 H), 7.02 (t, *J* = 7.5 Hz, 2 H), 6.95 (t, *J* = 7.4 Hz, 6 H), 6.77 (t, *J* = 7.4 Hz, 12 H) 4.03 (s, 3 H, OMe) ppm.

Synthesis of H₄LOMe. Under ambient conditions, a 100-mL round-bottom flask equipped with a stir bar was charged with S1 (1.4 g, 1.58 mmol, 1 equiv), trifluoroacetic acid (10 mL), and CH₂Cl₂ (20 mL). To the stirring brown solution, triethylsilane (1.0 mL, 6.34 mmol, 4 equiv) was added dropwise to form a light-yellow solution. A nitrogen inlet adapter was fitted onto the flask and the reaction was stirred at room temperature under nitrogen for 1 h. The yellow solution was dried *in vacuo* to yield a brown solid. The solid was washed with cold MeOH (100 mL) and cold diethyl ether (100 mL), then dried under vacuum to yield H₄LOMe as a pale brown solid that was carried forward without further purification (0.32 g, 49%). ¹H NMR (400 MHz, CDCl₃): δ 10.50 (s, 2 H), 8.36 (dd, *J* = 8.2, 1.2 Hz, 2 H), 8.01 (s, 2 H), 7.55 (d, *J* = 7.6 Hz, 2 H), 7.39 (t, *J* = 7.6 Hz, 2 H), 7.12 (td, *J* = 7.6, 1.3 Hz, 2 H), 4.05 (s, 3 H), 3.39 (s, 2 H) ppm.

Synthesis of [Et₄N]₂[LOMeZn]. In the glovebox, H₄LOMe (0.32 g, 0.78 mmol, 1 equiv) was added to an oven-dried 125-mL Erlenmeyer flask equipped with a stir bar. CH₃CN (40 mL) was added to the flask and the heterogeneous mixture was stirred for 5 min., then frozen in a liquid nitrogen-cooled cold well. The flask was removed from the cold well and allowed to thaw. While the mixture was thawing and stirring, NaHMDS (0.58 g, 3.14 mmol, 4 equiv) was added in parts as a solid. The yellow heterogeneous mixture was allowed to stir for 5 min. before [Et₄N]₂[ZnCl₄] (0.37 g, 0.78 mmol, 1 equiv) was added as a solid. The resulting yellow reaction mixture was allowed to stir at room temperature for 1 h. The yellow mixture was filtered through Celite and dried *in vacuo* to yield a dark yellow oil. The residue was dissolved in minimal CH₃CN and precipitated out as a yellow powder via layering of diethyl ether. The yellow powder was dried under vacuum

to yield $[\text{Et}_4\text{N}]_2[\text{LOMeZn}]$ (0.24 g, 41%). ^1H NMR (400 MHz, d_6 -DMSO): δ 7.57 (d, $J = 7.6$, 2 H), 7.46 (s, 2 H), 7.14 (d, $J = 7.6$, 2 H), 6.64 (t, $J = 7.4$, 2 H), 6.50 (t, $J = 7.4$, 2 H), 3.99 (s, 3 H), 3.11 (q, $J = 7.2$ Hz, 16 H), 1.08 (t, $J = 7.2$ Hz, 24 H) ppm. ^{13}C NMR (101 MHz, d_6 -DMSO): δ 169.83, 160.96, 153.54, 147.03, 145.59, 130.71, 122.43, 119.76, 118.94, 105.67, 55.89, 51.35, 7.01 ppm.

Synthesis of $[\text{Et}_4\text{N}]_2[\mathbf{3}]$ and $[\text{Et}_4\text{N}]_2[\mathbf{2}]$. In the glovebox, $[\text{Et}_4\text{N}]_2[\mathbf{1}]$ (0.100 g, 0.125 mmol, 1 equiv) was added to a scintillation vial equipped with a stir bar and dissolved in DMSO (1 mL). DMAD (17 μL , 0.138 mmol, 1.1 equiv) was added via syringe, and the solution mixture rapidly became dark red. The homogeneous solution was allowed to stir for 20 h at room temperature. Diethyl ether (20 mL) was added to the solution to yield a dark red oily precipitate. The supernatant was decanted off and the residue was washed with additional diethyl ether (20 mL). Acetone (6 mL) was added to the residue to extract $[\text{Et}_4\text{N}]_2[\mathbf{3}]$. The dark red acetone fraction was filtered through Celite and set up to crystallize via vapor diffusion of diethyl ether to yield $[\text{Et}_4\text{N}]_2[\mathbf{3}]$ as a red solid (0.031 g, 67%, ca. 87% by ^1H NMR). Additional attempts to crystallize did not result in a high bulk purity. $[\text{Et}_4\text{N}]_2[\mathbf{3}]$ ^1H NMR (400 MHz, d_6 -DMSO): δ 3.51 (s, 12 H), 3.18 (q, $J = 7.2$ Hz, 16 H), 1.14 (t, $J = 7.2$ Hz, 24 H) ppm. ^{13}C NMR (101 MHz, d_6 -DMSO): δ 169.71, 135.99, 51.40, 51.07, 7.07 ppm. UV-Vis: 364 nm ($14100 \text{ M}^{-1} \text{ cm}^{-1}$), 488 nm ($4800 \text{ M}^{-1} \text{ cm}^{-1}$), 508 nm ($4800 \text{ M}^{-1} \text{ cm}^{-1}$) HRMS (ESI m/z): calcd. for $\text{C}_{12}\text{H}_{13}\text{O}_8\text{S}_4\text{Zn}$ 476.8785. Found: 476.8620 $[\text{M}+\text{H}]$.

CH_3CN (5 mL) was added to the remaining solid residue and the dark red mixture was filtered through Celite. The filtrate was set up to crystallize via vapor diffusion of diethyl ether into the acetonitrile solution. After 16 h., the red supernatant was decanted off and the pale-yellow crystals were washed with cold CH_3CN (2 mL) and diethyl ether (4 mL) to yield $[\mathbf{2}]^{2-}$ (0.043 g, 60%). $[\text{Et}_4\text{N}]_2[\mathbf{2}]$ ^1H NMR (400 MHz, d_6 -DMSO): δ 7.94 (m, 6 H), 7.50 (d, $J = 7.5$ Hz, 4 H), 6.65 (m, 8 H), 6.52 (t, $J = 7$ Hz, 4 H), 3.18 (q, $J = 7.1$ Hz, 16 H), 1.14 (t, $J = 7.1$ Hz, 24 H) ppm. ^{13}C NMR (101 MHz, d_6 -DMSO): δ 161.92, 153.69, 150.49, 139.62, 132.90, 130.93, 126.89, 122.83, 121.37, 121.24, 51.36, 7.04 ppm. UV-Vis: 330 nm ($18900 \text{ M}^{-1} \text{ cm}^{-1}$). HRMS (ESI m/z): calcd. for $\text{C}_{38}\text{H}_{23}\text{N}_6\text{O}_4\text{S}_6\text{Zn}$ 882.9396. Found: 882.9294 $[\text{M}+\text{H}]$. Anal. Calcd. for $\text{C}_{54}\text{H}_{62}\text{N}_8\text{O}_4\text{S}_6\text{Zn}$: C, 56.65; H, 5.46; N, 9.79. Found: C, 55.69; H, 5.65; N, 10.46. This discrepancy in elemental analysis may be due to residual acetonitrile in the crystal lattice.

Synthesis of $\text{H}_2\text{L}^{\text{S3}}$.

In the glovebox, a Schlenk tube equipped with a stir bar was charged with H_4L (0.300 g, 0.786 mmol, 1 equiv) and THF (30 mL). The flask was sealed with a Teflon stopper and removed from the glovebox and cooled to -78 $^\circ\text{C}$. The Teflon stopper was removed under nitrogen flow and replaced with a rubber septum. Triethylamine (0.24 mL, 1.73 mmol, 2.2 equiv) was added via syringe and the resulting yellow mixture was allowed to stir for 5 min. SCL_2 (0.05 mL, 0.865 mmol, 1.1 equiv) was added dropwise via syringe, forming a cloudy orange mixture that slowly turned cloudy white after stirring for 1 h at -78 $^\circ\text{C}$. The mixture was removed from the bath after 1 h and allowed to warm to room temperature before pouring into water (50 mL). CHCl_3 (150 mL) was

added and the organic phase was collected, dried over MgSO_4 , filtered, and dried *in vacuo* to yield a white powder (0.29 g, 90%). ^1H NMR (400 MHz, CDCl_3): δ 11.64 (s, 2 H), 8.65 (d, $J = 7.6$ Hz, 2 H), 8.48 (d, $J = 7.8$ Hz, 2 H), 8.22 (t, $J = 7.8$ Hz, 1 H), 7.65 (d, $J = 7.8$ Hz, 2 H), 7.53 (t, $J = 7.8$ Hz, 2 H), 7.21 (t, $J = 7.6$ Hz, 2 H) ppm. HRMS (ESI m/z): calcd. for $\text{C}_{19}\text{H}_{14}\text{N}_3\text{O}_2\text{S}_3$ 412.0248. Found: 412.0224 [M+H].

Characterization

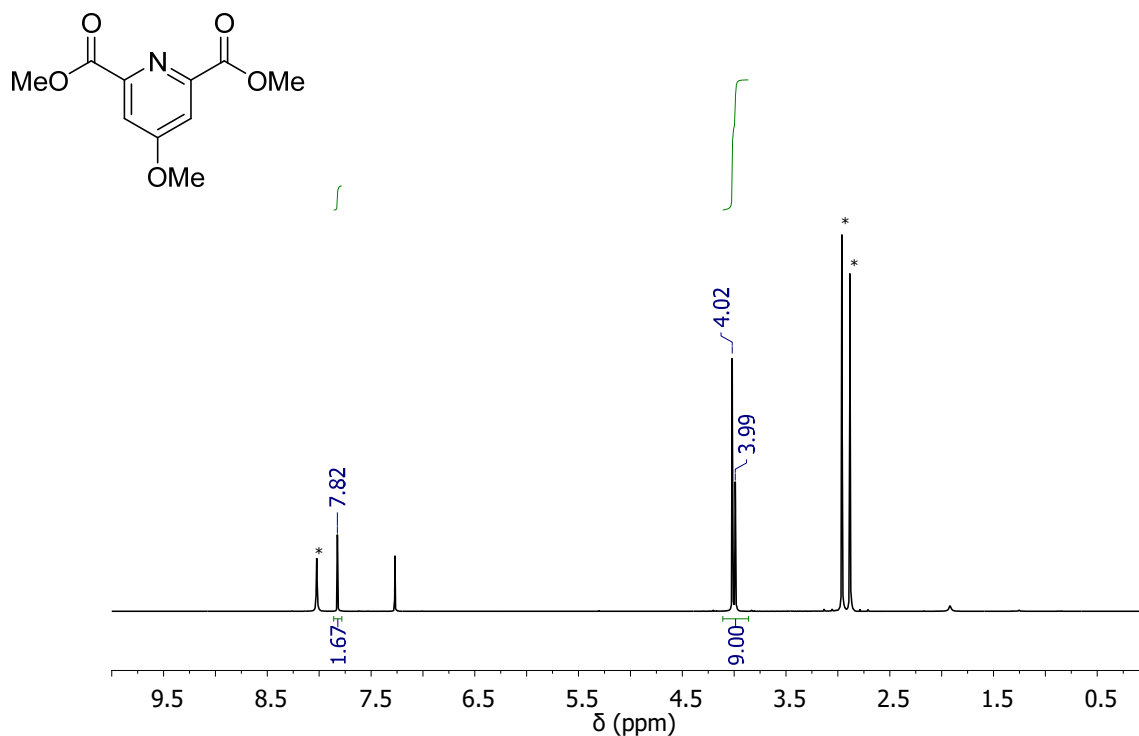


Figure S1. ^1H NMR spectrum of dimethyl 4-methoxypyridine-2,6-dicarboxylate in CDCl_3 at 25 $^\circ\text{C}$. DMF is also present (*).

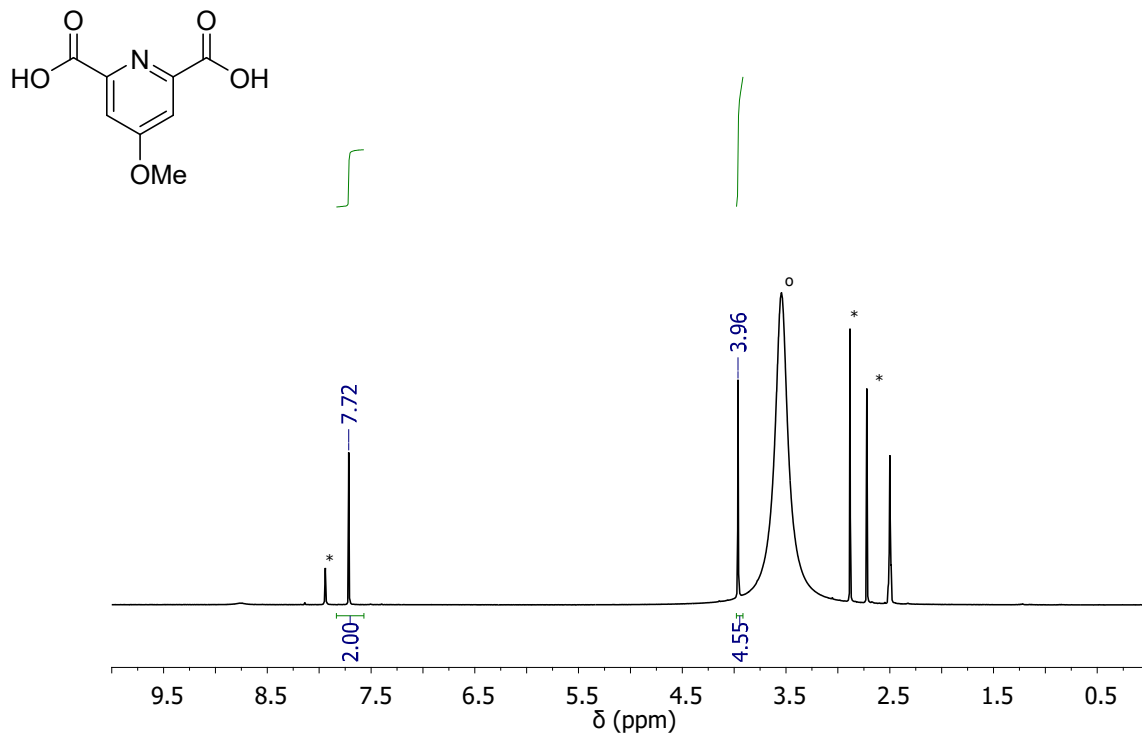


Figure S2. ^1H NMR spectrum of 4-methoxypyridine-2,6-dicarboxylic acid in d_6 -DMSO at 25 °C. DMF (*) and water (o) are also present.

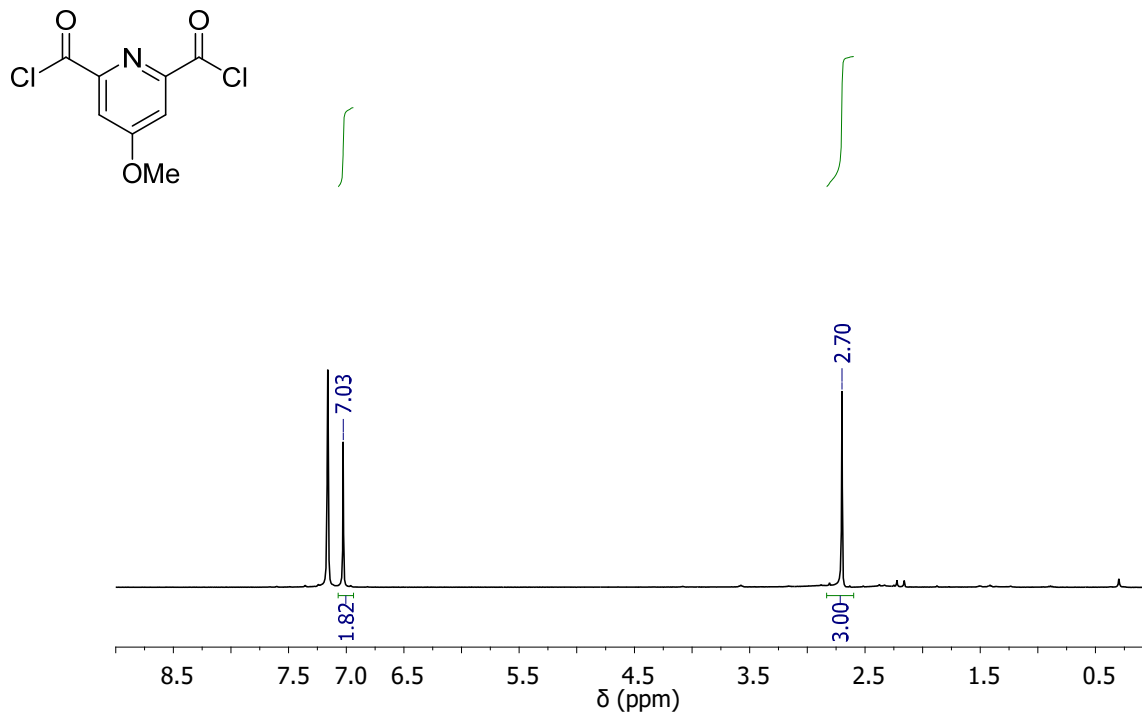


Figure S3. ^1H NMR spectrum of 4-methoxypyridine-2,6-dicarbonyl chloride in C_6D_6 at 25 °C.

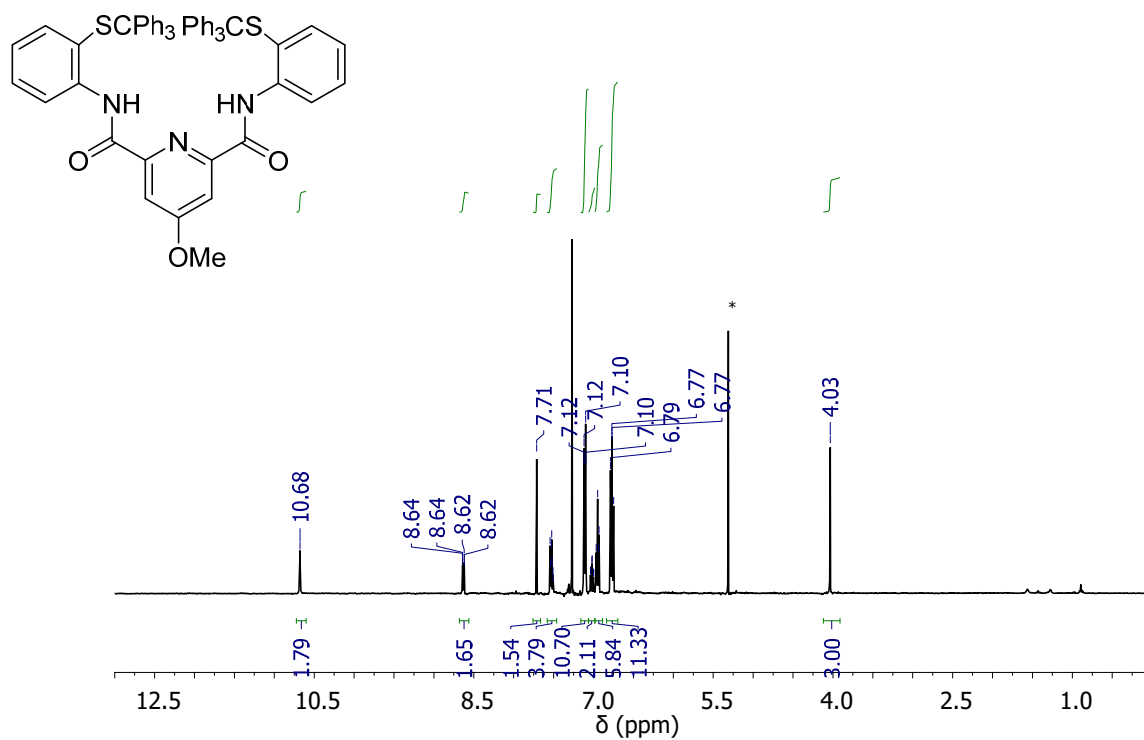


Figure S4. ¹H NMR spectrum of S1 in CDCl₃ at 25 °C. CH₂Cl₂ (*) is also present.

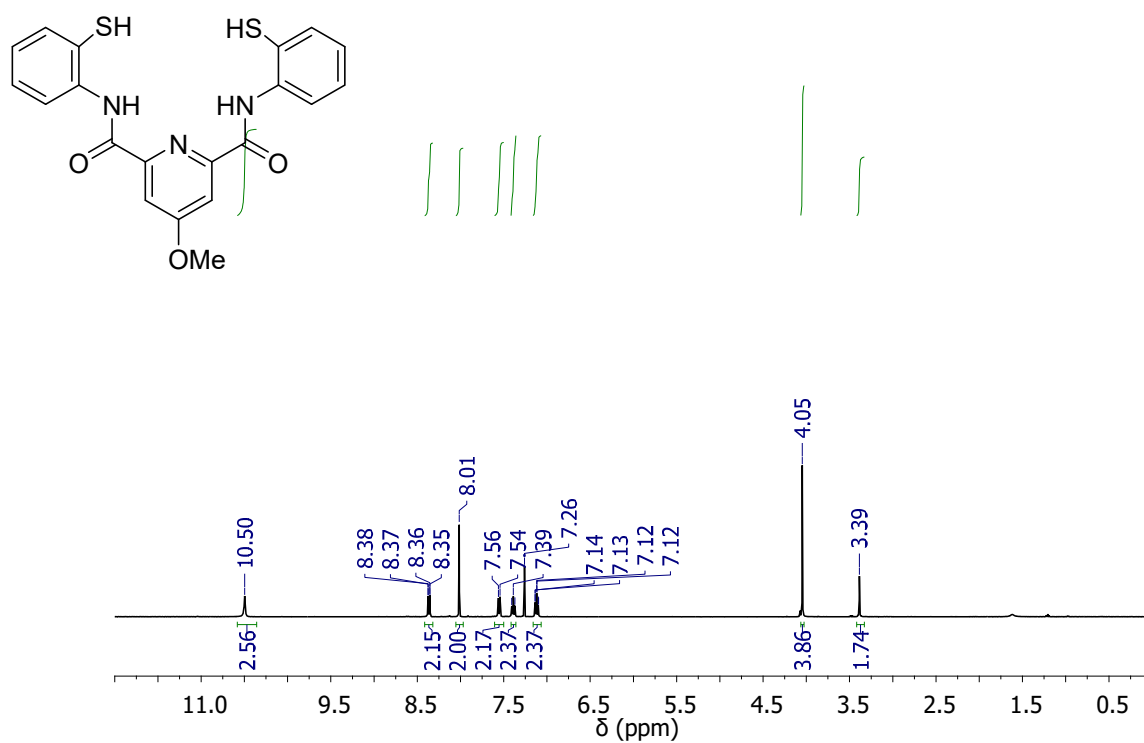


Figure S5. ¹H NMR spectrum of H4LOMe in CDCl₃ at 25 °C.

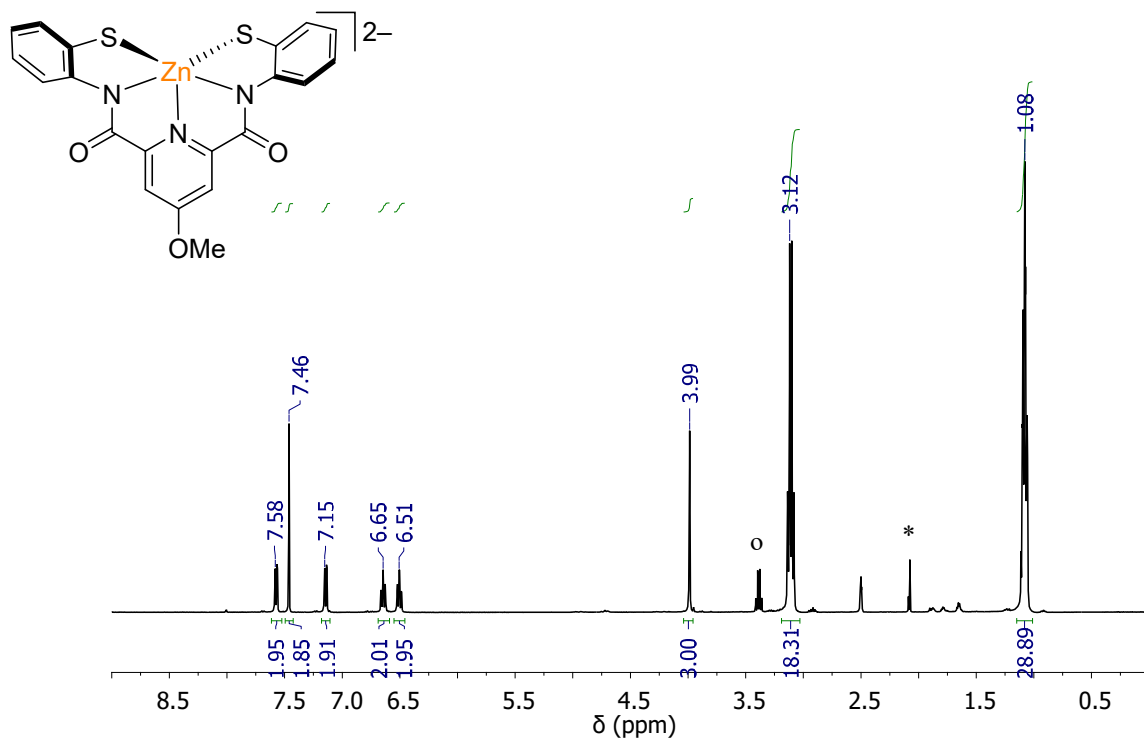


Figure S6. 1H NMR spectrum of $[Et_4N]_2[LOMeZn]$ in d_6 -DMSO at 25 °C. CH₃CN (*) and diethyl ether (o) are also present.

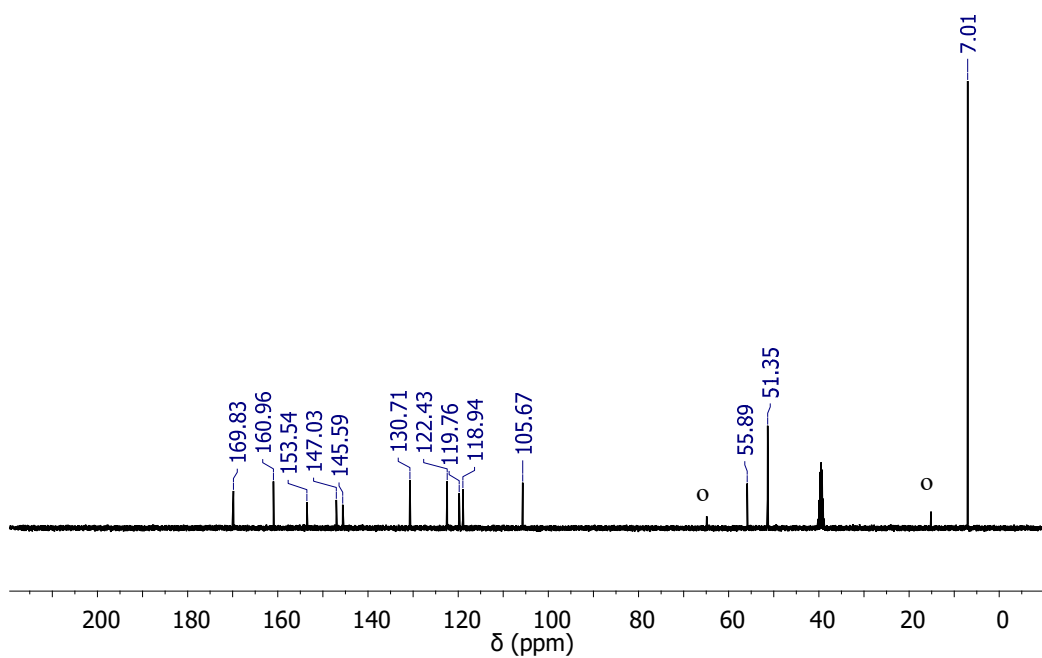


Figure S7. ^{13}C NMR spectrum of $[Et_4N]_2[LOMeZn]$ in d_6 -DMSO at 25 °C. Diethyl ether (o) is also present.

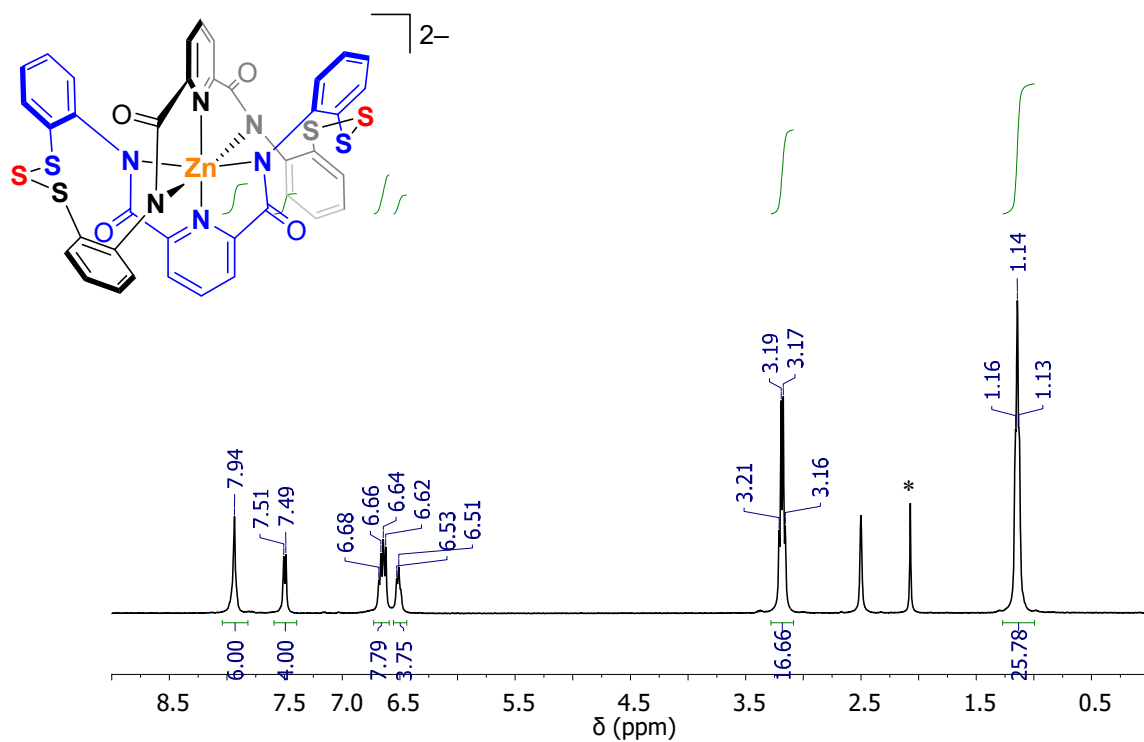


Figure S8. ¹H NMR spectrum of [Et₄N]₂[2] in *d*₆-DMSO at 25 °C. CH₃CN (*) is also present.

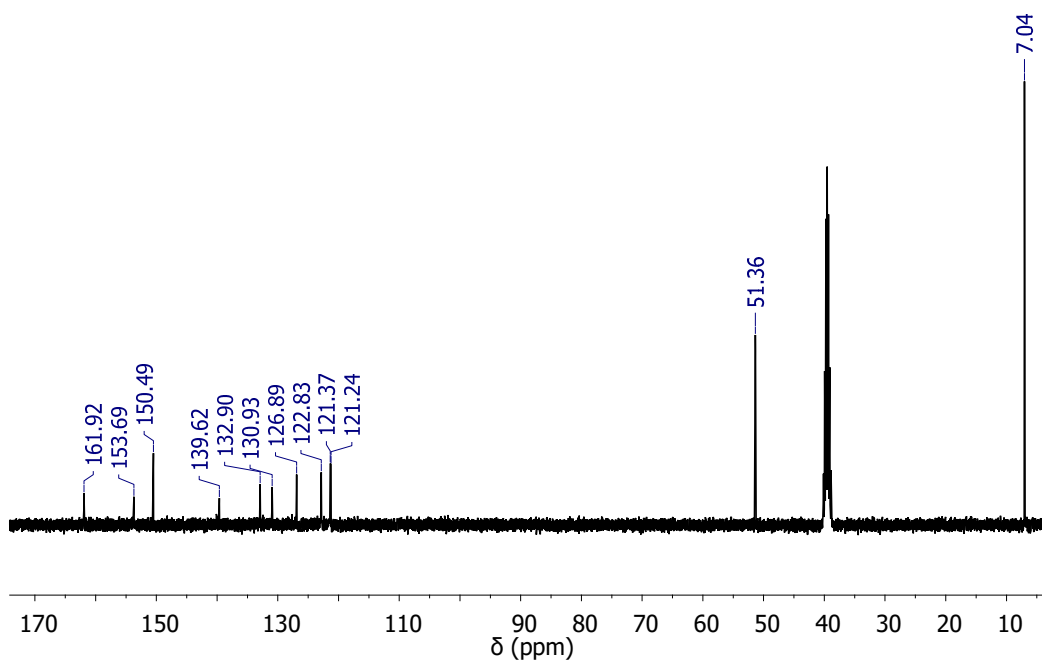


Figure S9. ¹³C NMR spectrum of [Et₄N]₂[2] in *d*₆-DMSO at 25 °C.

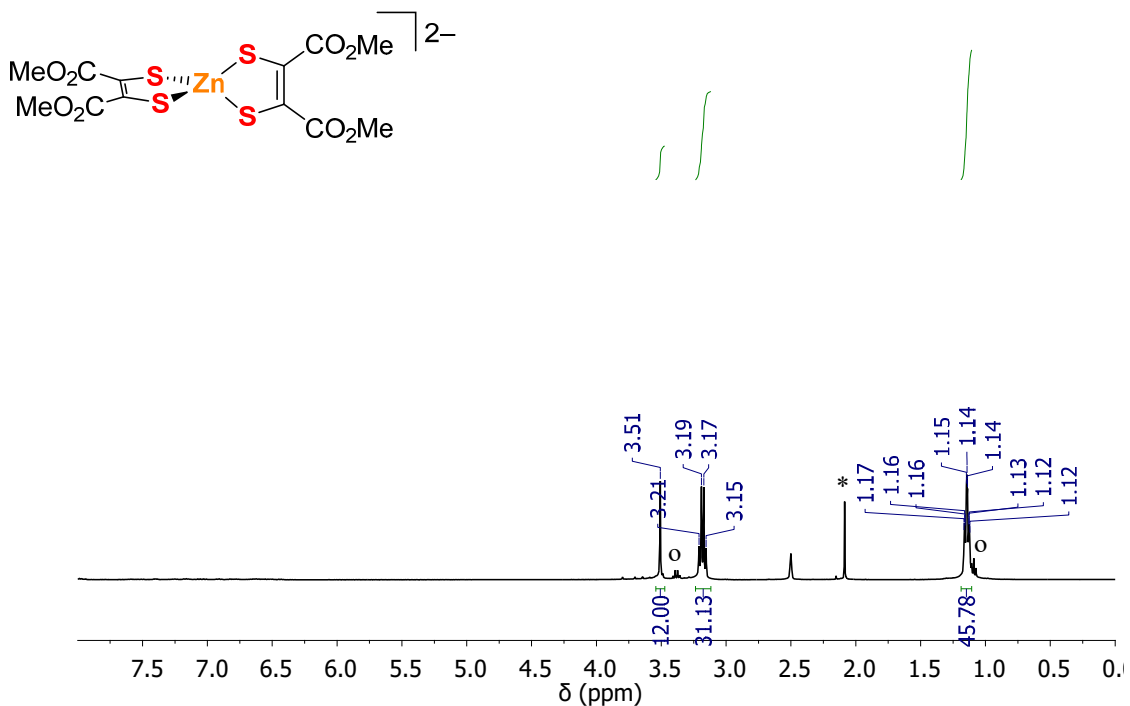


Figure S10. ^1H NMR spectrum of $[\text{Et}_4\text{N}]_2[\mathbf{3}]$ in d_6 -DMSO at 25 °C. CH_3CN (*) and diethyl ether (o) are also present.

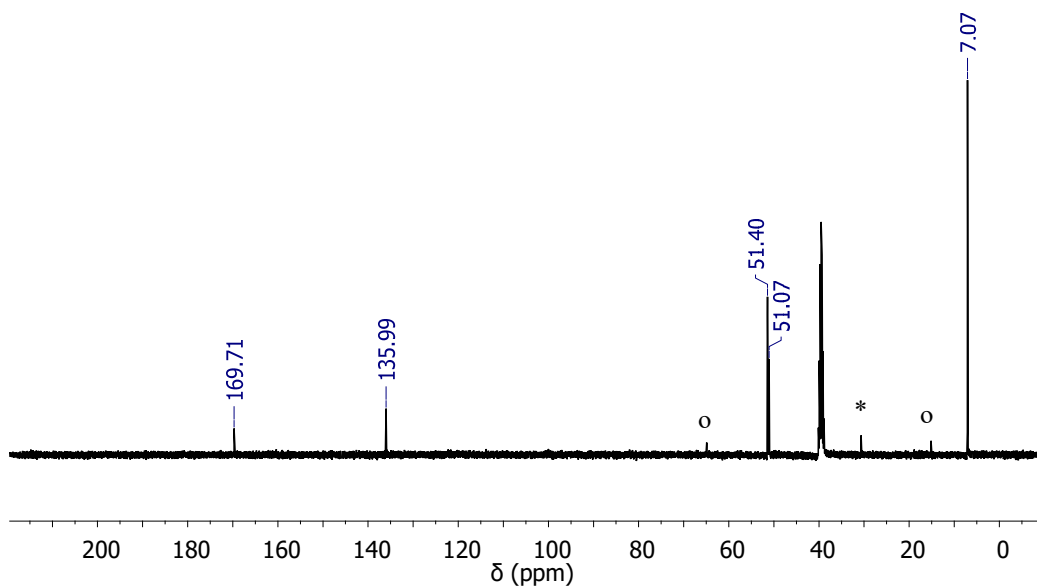


Figure S11. ^{13}C NMR spectrum of $[\text{Et}_4\text{N}]_2[\mathbf{3}]$ in d_6 -DMSO at 25 °C. Diethyl ether (o) and acetone (*) are also present.

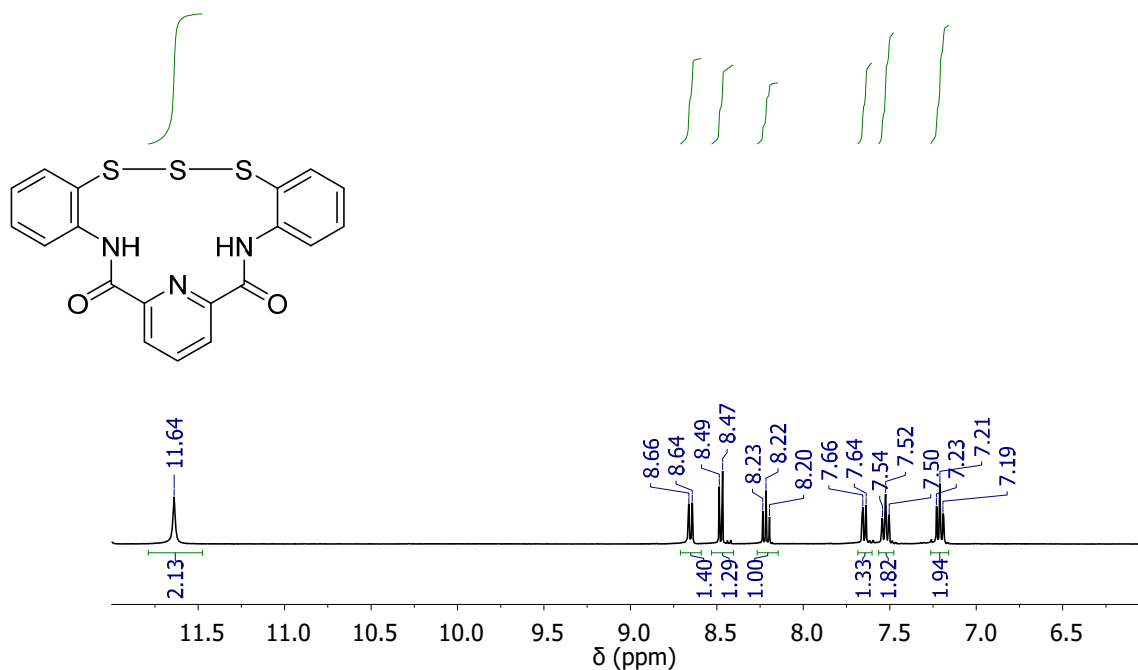


Figure S12. 1H NMR spectrum of H_2LS^3 in $CDCl_3$ at 25 °C.

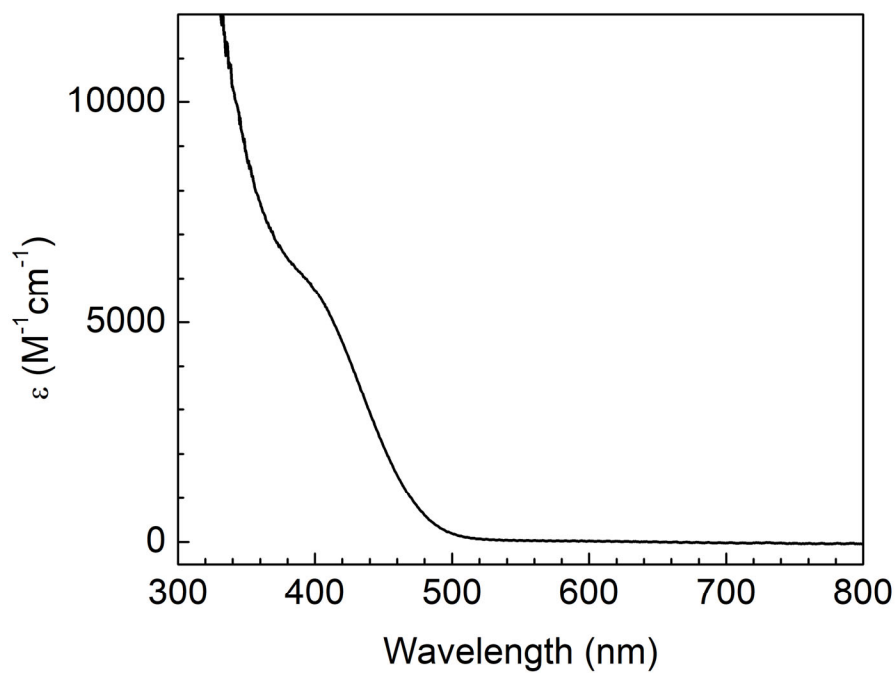


Figure S13. Electronic absorption spectrum of $[Et_4N]_2[1]$ in CH_3CN .

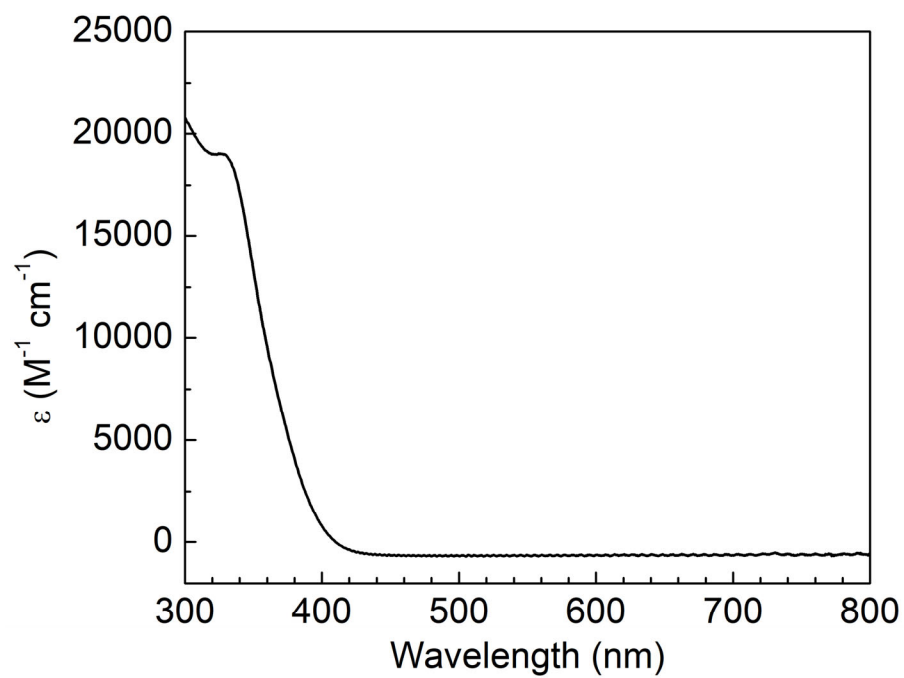


Figure S14. Electronic absorption spectrum of [Et₄N]₂[2] in CH₃CN.

Reactions

Sulfur Transfer from $[\text{Et}_4\text{N}]_2[\mathbf{1}]$ to $[\text{Et}_4\text{N}]_2[\text{LOMeZn}]$.

In the glovebox, $[\text{Et}_4\text{N}]_2[\mathbf{1}]$ (0.010 g, 0.013 mmol, 1 equiv) was dissolved in d_6 -DMSO (0.6 mL) and added to a screw-cap NMR tube that was then sealed with a septum. In a scintillation vial, $[\text{Et}_4\text{N}]_2[\text{LOMeZn}]$ (0.009 g, 0.013 mmol, 1 equiv) was dissolved in d_6 -DMSO (0.4 mL) and taken up into a syringe. After collecting a ^1H NMR spectrum of $[\mathbf{1}]^{2-}$, the solution of $[\text{Et}_4\text{N}]_2[\text{LOMeZn}]$ was added via syringe to the NMR tube to yield a dark green solution. A ^1H NMR spectrum was collected within 1 min. of injection to demonstrate fast sulfur exchange between complexes.

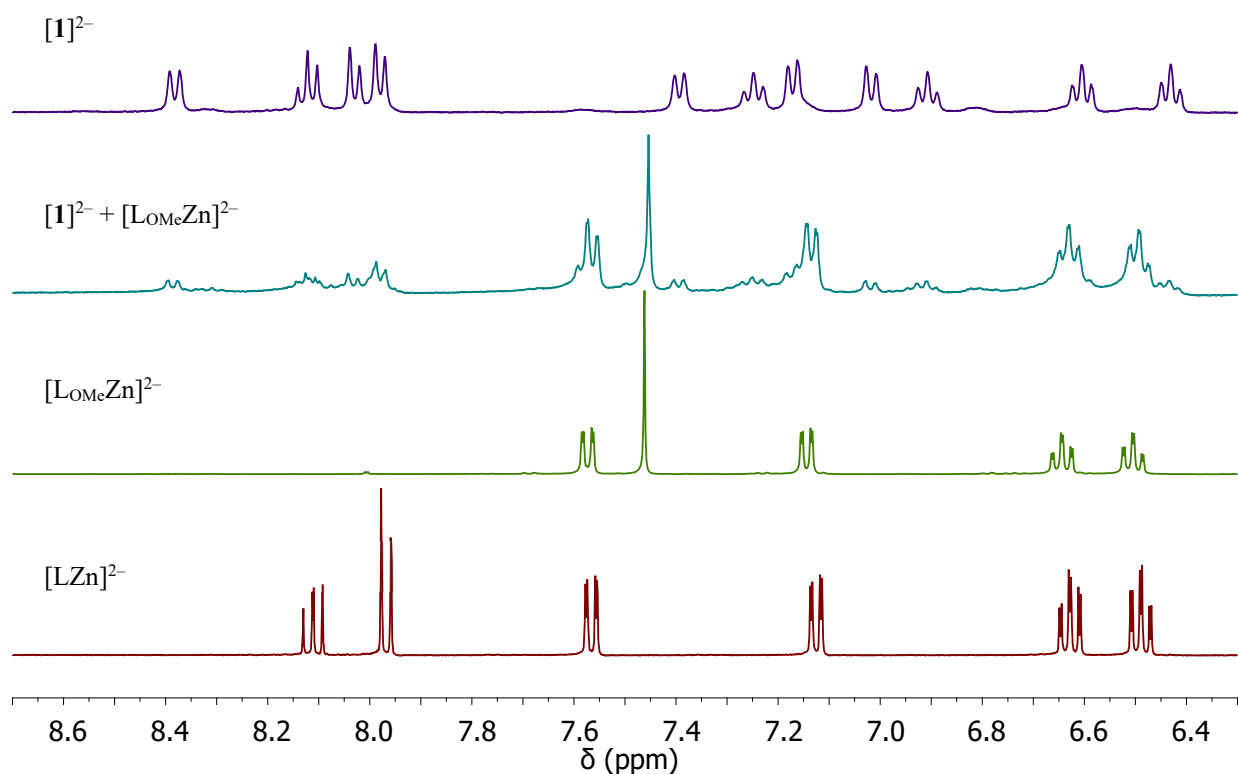


Figure S15. ^1H NMR spectra of $[\text{Et}_4\text{N}]_2[\mathbf{1}]$, a 1:1 mixture of $[\text{Et}_4\text{N}]_2[\mathbf{1}]$ and $[\text{Et}_4\text{N}]_2[\text{LOMeZn}]$, $[\text{Et}_4\text{N}]_2[\text{LOMeZn}]$, and $[\text{Et}_4\text{N}]_2[\text{LZn}]$ in d_6 -DMSO at 25 $^\circ\text{C}$.

Sulfur transfer from $(\text{TMEDA})\text{ZnS}_6$ to $[\text{Et}_4\text{N}]_2[\text{LZn}]$.

In the glovebox, $[\text{Et}_4\text{N}]_2[\text{LZn}]$ (0.020 g, 0.028 mmol, 1 equiv) was added to a scintillation vial and dissolved in d_6 -DMSO (0.6 mL). $(\text{TMEDA})\text{ZnS}_6$ (0.007 g, 0.028 mmol, 1 equiv) was added to the solution as a solid, and the mixture was transferred to an NMR tube. A ^1H NMR spectrum was collected that showed complete conversion to $[\mathbf{1}]^{2-}$ within minutes of addition.

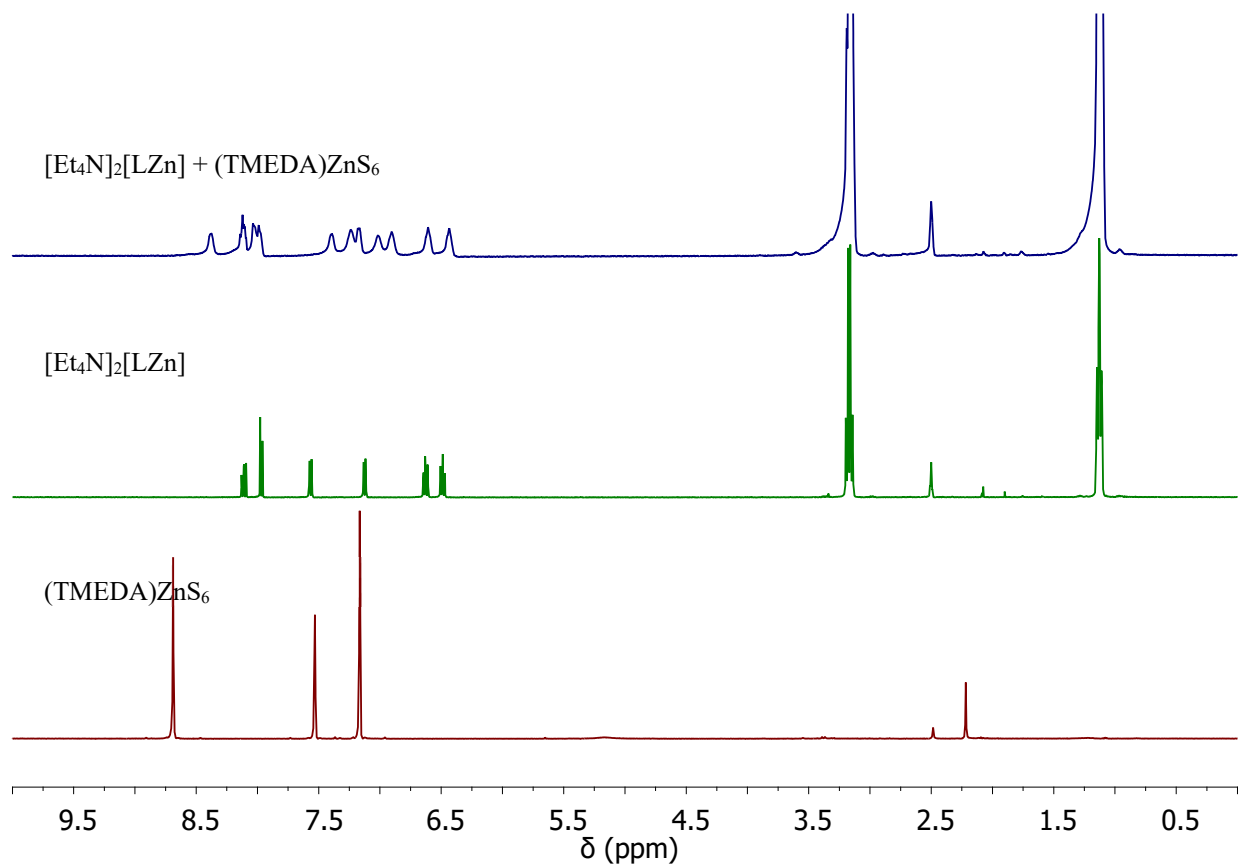


Figure S16. ^1H NMR spectra of a mixture of $(\text{TMEDA})\text{ZnS}_6$ and $[\text{Et}_4\text{N}]_2[\text{LZn}]$ in d_6 -DMSO, $[\text{Et}_4\text{N}]_2[\text{LZn}]$ in d_6 -DMSO, and $(\text{TMEDA})\text{ZnS}_6$ in d_5 -pyridine at 25°C .

Methylation of $[\text{Et}_4\text{N}]_2[\mathbf{1}]$ with one equivalent of methyl iodide.

In the glovebox, $[\text{Et}_4\text{N}]_2[\mathbf{1}]$ (0.020 g, 0.025 mmol, 1 equiv) was dissolved in d_6 -DMSO (0.6 mL) and added to a screw-cap NMR tube and taken out of the glovebox. Methyl iodide (1.7 μL , 0.028 mmol, 1.1 equiv) was injected via syringe and the NMR tube was inverted several times. A ^1H NMR spectrum was collected within 15 minutes after addition of methyl iodide.

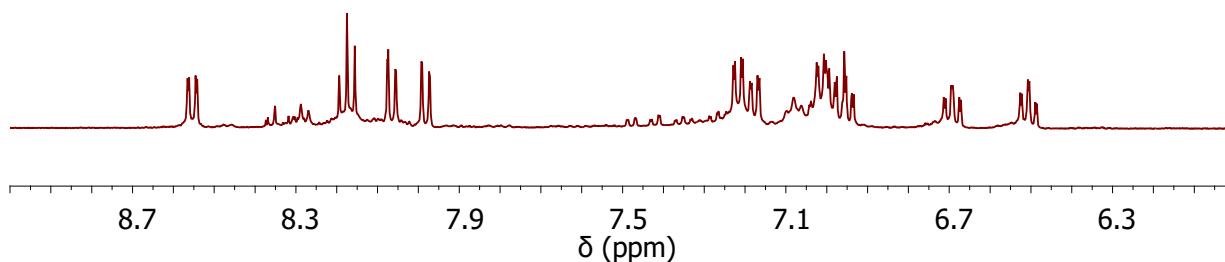
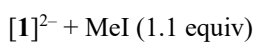
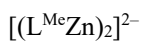


Figure S17. 1H NMR spectra of $[Et_4N]_2[(L^{Me}Zn)_2]$ (top) and a mixture of $[Et_4N]_2[1]$ and methyl iodide (1.1 equiv) (bottom) in d_6 -DMSO at 25 °C.

Methylation of $[Et_4N]_2[1]$ with two equivalents of methyl iodide.

In the glovebox, $[Et_4N]_2[1]$ (0.020 g, 0.025 mmol, 1 equiv) was dissolved in d_6 -DMSO (0.6 mL) and added to a screw-cap NMR tube and taken out of the glovebox. Methyl iodide (3.4 μ L, 0.055 mmol, 2.2 equiv) was injected via syringe and the NMR tube was inverted several times. A 1H NMR spectrum was collected within 15 minutes after addition of methyl iodide.

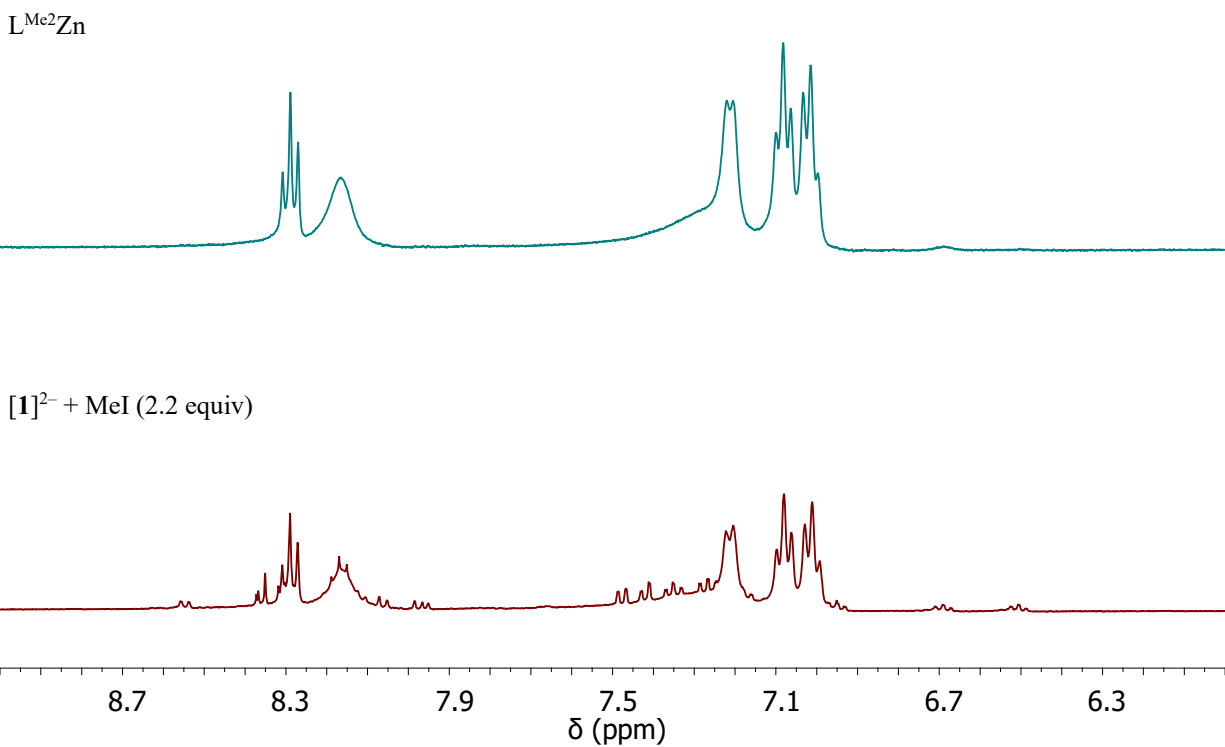


Figure S18. ^1H NMR spectrum of $\text{L}^{\text{Me}_2}\text{Zn}$ (top) and a mixture of $[\text{Et}_4\text{N}]_2[\mathbf{1}]$ and methyl iodide (2.2 equiv) (bottom) in d_6 -DMSO at 25 °C.

Methylation of Intermediate A

In the glovebox, $[\text{Et}_4\text{N}]_2[\mathbf{1}]$ (0.070 g, 0.088 mmol, 1 equiv) was dissolved in 0.6 mL DMSO and added to a screw-cap NMR tube. DMAD (12 μL , 0.096 mmol, 1.1 equiv) was added via syringe, and the NMR tube was inverted several times to mix the solution. The NMR tube was removed from the glovebox, and MeI (10 μL , 0.160 mmol, 1.8 equiv) was added via syringe within 10 min. of DMAD addition. The NMR tube was returned to the glovebox and the dark green-brown solution was added to a scintillation vial. Diethyl ether (20 mL) was added to the solution to yield a brown oily precipitate. The mother liquor was decanted and the oily precipitate was washed with diethyl ether (20 mL). The brown residue was washed with THF (3 mL), then redissolved in DMF (1 mL) and filtered through Celite. The DMF solution was dried *in vacuo* to yield a brown powder that could not be separated from Et_4NI .

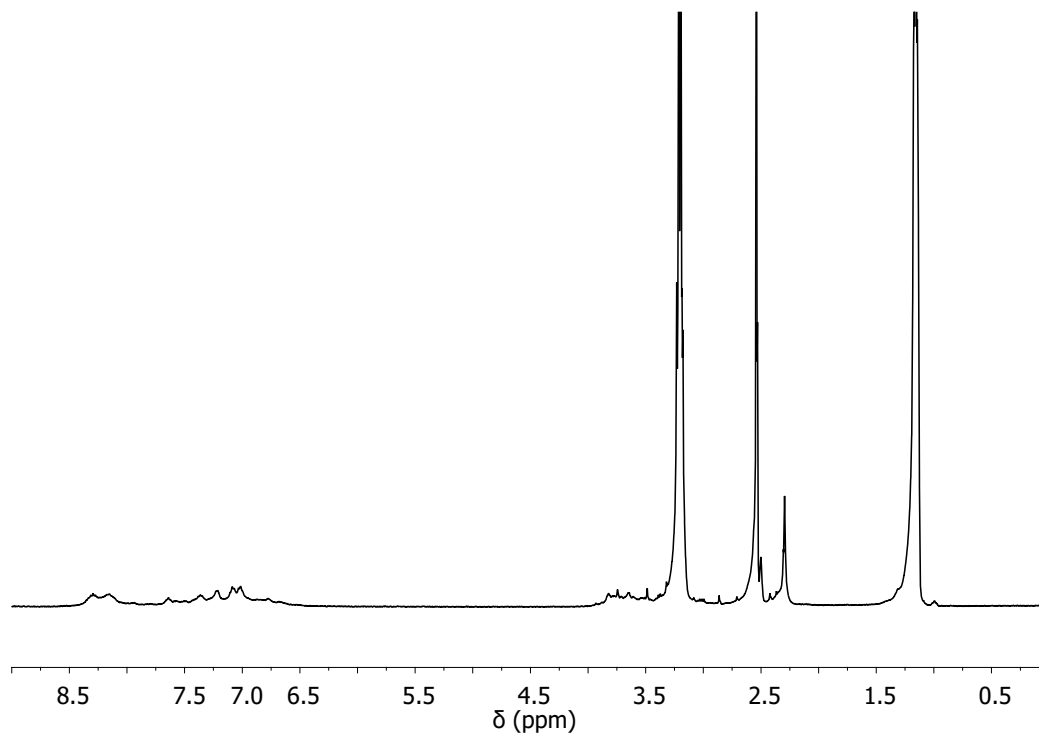


Figure S19. ^1H NMR spectrum of a mixture of **A** and methyl iodide (1.8 equiv) in d_6 -DMSO at 25 °C.

Treatment of A with water.

In the glovebox, $[\text{Et}_4\text{N}]_2[\mathbf{1}]$ (0.100 g, 0.125 mmol, 1 equiv) was added to a scintillation vial equipped with a stir bar and dissolved in 1 mL DMSO. DMAD (17 μL , 0.138 mmol, 1.1 equiv) was added via syringe while stirring. The scintillation vial was capped then removed from the glovebox before water (10 mL) was added to the red solution to give a cloudy orange-yellow mixture. The mixture was added to a separatory funnel and brine (10 mL) was added to the mixture before extracting with CH_2Cl_2 (10 mL) and CHCl_3 (10 mL). The organic fractions were combined and dried with MgSO_4 prior to filtering and drying in vacuo to yield an orange-red oily residue. The residue was dissolved in CDCl_3 and a ^1H NMR spectrum was collected. The ^1H NMR spectrum matched closely with previously observed ligand oxidation so no further workup was performed.

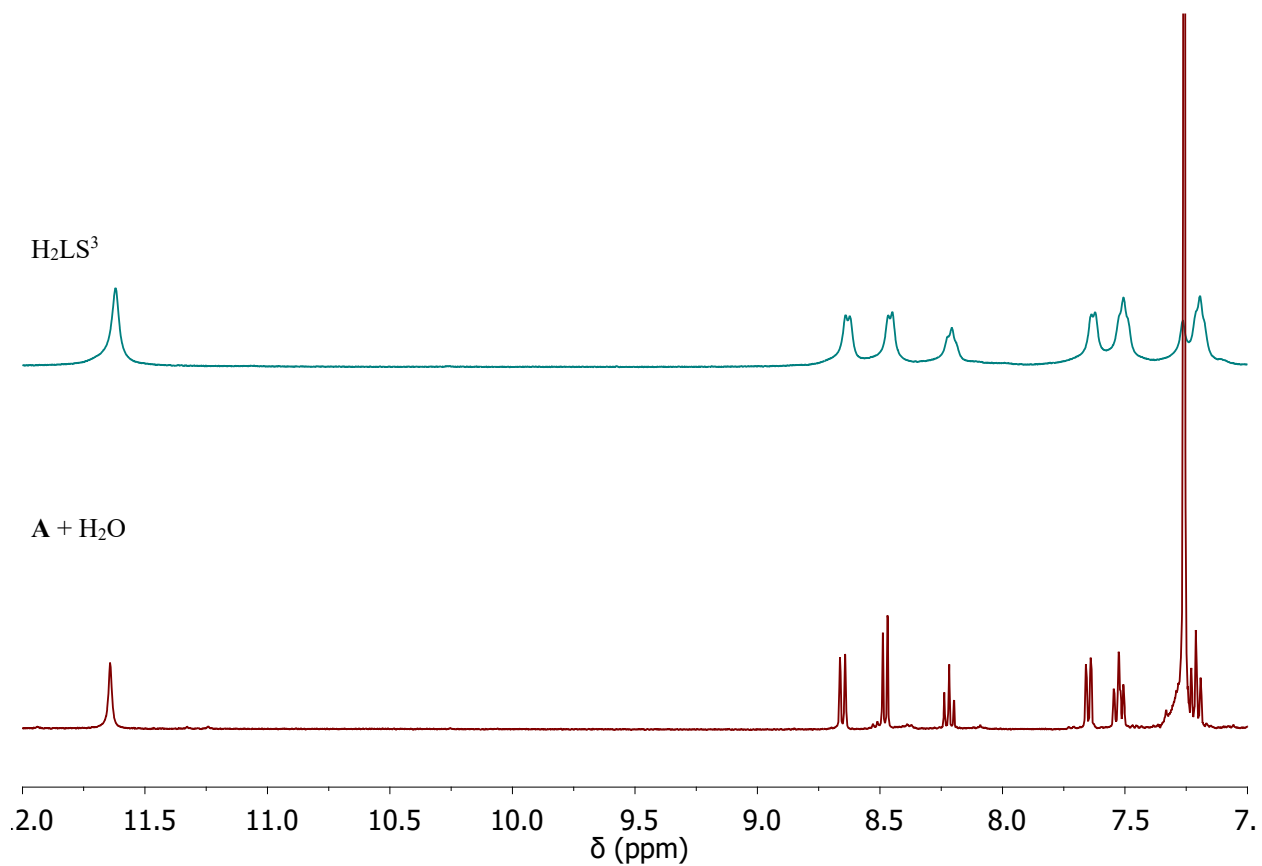
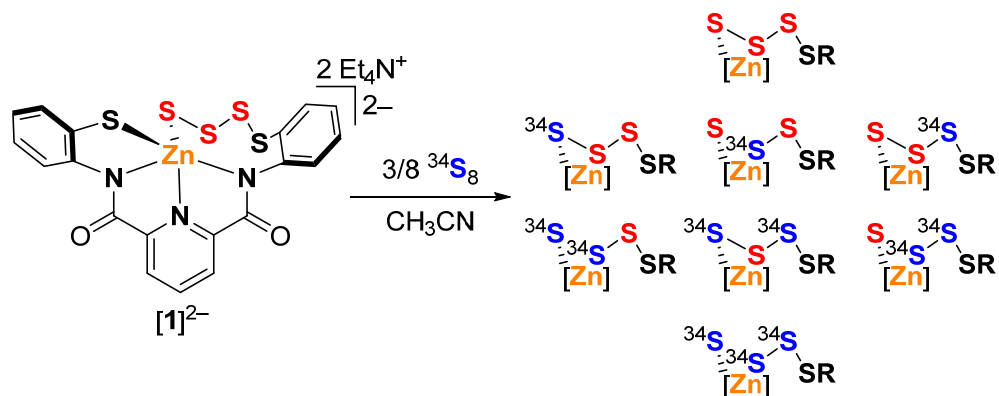


Figure S20. ¹H NMR spectra of H₂LS³ (top) and the organic product obtained after treatment of **A** with water in CDCl₃ at 25 °C.

³⁴S exchange of [Et₄N]₂[**1**].

In the glovebox, [Et₄N]₂[**1**] (0.020 g, 0.025 mmol, 1 equiv) was dissolved in CH₃CN (5 mL), and ³⁴S₈ (0.003 g, 0.009 mmol, 3/8 equiv) was added as a solid. The mixture was allowed to stir for 0.25 h before an aliquot (0.1 mL) was removed and diluted to a 10⁻⁶ M solution in CH₃CN. This process was followed to remove a second and third aliquot after stirring the mixture for 2 h and 4 h, respectively. The aliquots taken at 2 and 4 hours were identical and matched closely with a simulation of a statistical mixture of scrambling at all tetrasulfanido sulfur atoms (possible scrambling products shown in Scheme S2).



Scheme S2. Representation of the possible products obtained via scrambling of tetrasulfanido moiety with ^{34}S .

$^{34}\text{S}_8$ exchange with natural abundance S_8 . In the glovebox, $^{34}\text{S}_8$ (0.004 g, 0.015 mmol, 1 equiv) was added to a 2 mL screw cap vial. CH_3CN (2 mL) was added to the vial before sealing the vial with a screw cap. S_8 (0.004 g, 0.015 mmol, 1 equiv) was added to a separate 2 mL vial and CH_3CN (2 mL) was added to the vial before sealing with a screw cap. EI-MS spectra were recorded for each solution. Equal volumes of each solution were taken up and combined in a separate vial in air. An EI-MS spectrum was recorded two hours after combination of the two solutions.

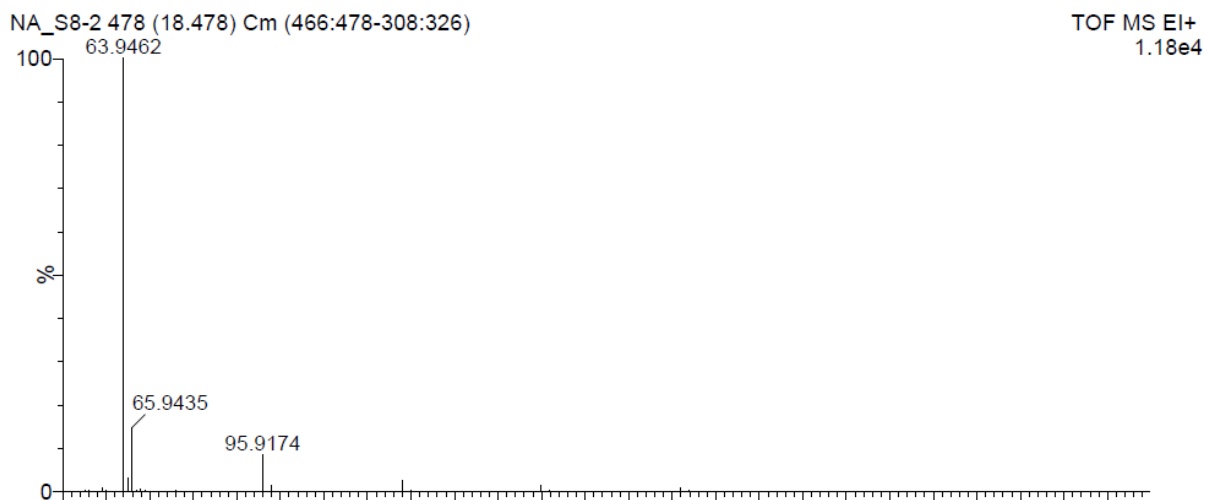


Figure S21. EI mass spectrum of natural abundance sulfur in CH_3CN . The lowest m/z values correspond to S_2^+ ions.

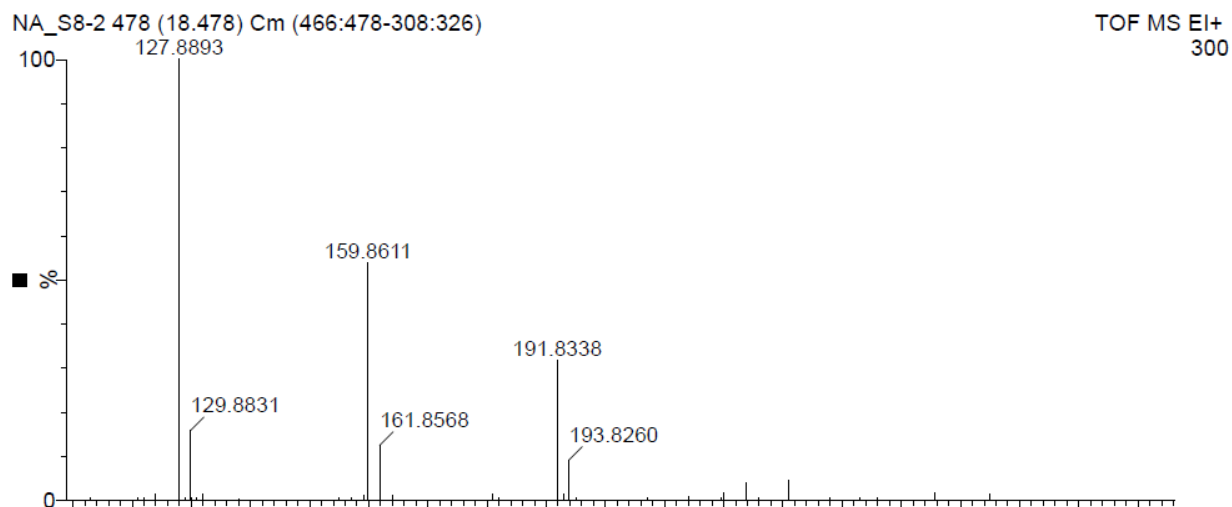


Figure S22. EI mass spectrum of natural abundance sulfur in CH₃CN. The picked m/z peaks correspond to S₄⁺-S₆⁺ ions.

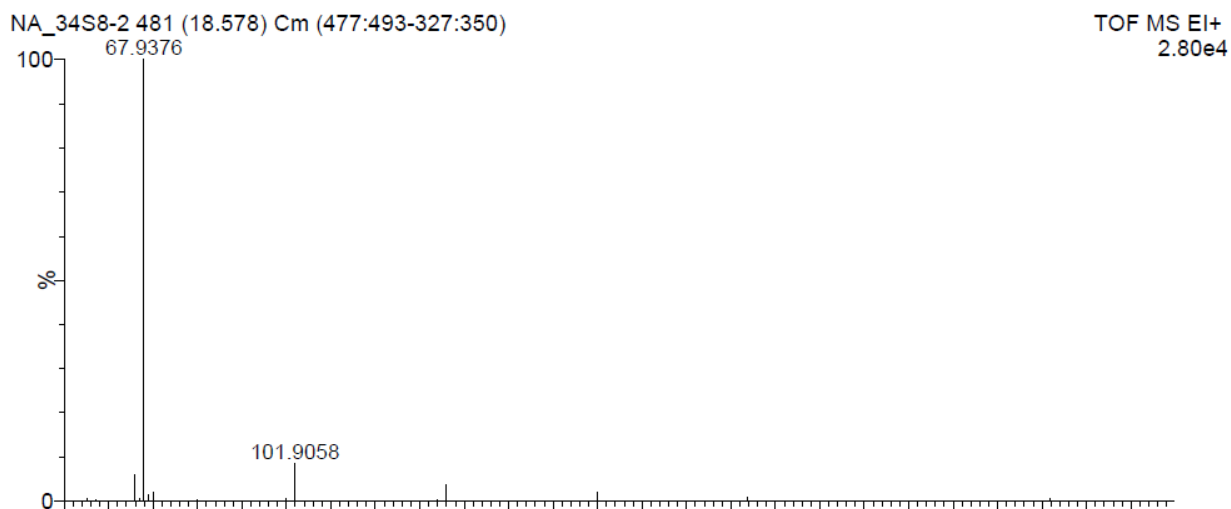


Figure S23. EI mass spectrum of ³⁴S₈ in CH₃CN. The lowest m/z values correspond to S₂⁺ ions.

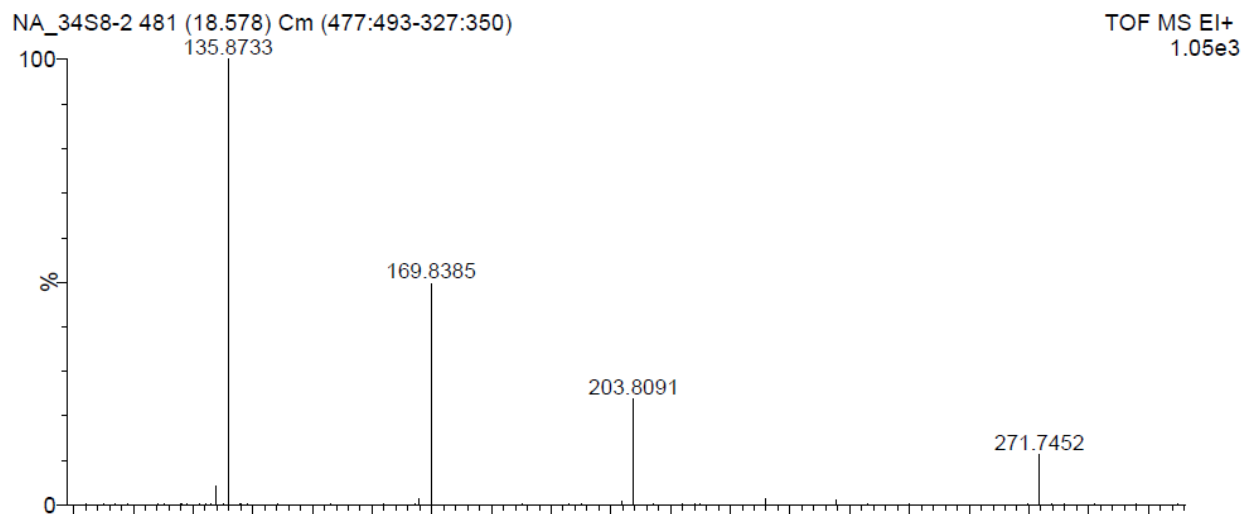


Figure S24. EI mass spectrum of $^{34}\text{S}_8$ in CH_3CN . The picked m/z peaks correspond to S_4^+ - S_6^+ , and S_8^+ ions.

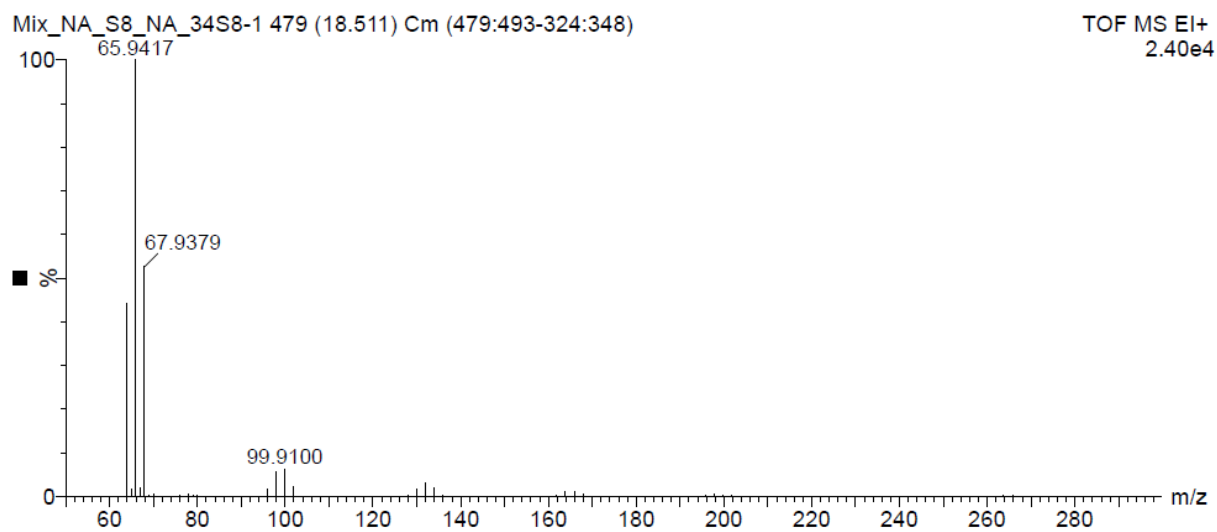


Figure S25. EI mass spectrum of combined natural abundance S_8 and $^{34}\text{S}_8$ in CH_3CN . The lowest m/z values correspond to S_2^+ ions.

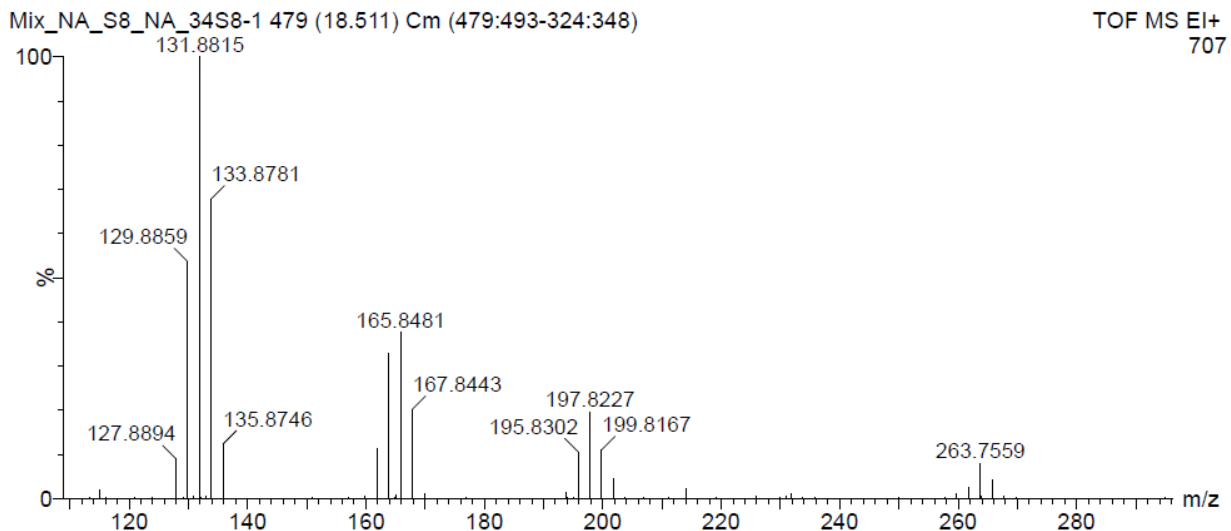


Figure S26. EI mass spectrum of combined natural abundance S_8 and $^{34}S_8$ in CH_3CN . The picked m/z peaks correspond to S_4^+ - S_6^+ , and S_8^+ ions.

Kinetics measurements of the reaction of $[Et_4N]_2[1]$ with DMAD.

In the glovebox, a 5.0×10^{-4} M solution of $[Et_4N]_2[1]$ in CH_3CN (4 mL) was added to a quartz Schlenk cuvette with a sidearm reagent reservoir charged with a CH_3CN solution of DMAD (0.4 mL, 5.0×10^{-3} M). The sealed cuvette was removed from the glovebox and a spectrum of the solution of $[Et_4N]_2[1]$ prior to mixing with DMAD was collected. DMAD was added by opening the reservoir and shaking the cuvette for 10 s. The cuvette was returned to the spectrometer and spectra were recorded every 18 seconds for 20 min. then every 5 min. for 24 h (Fig. S26). The same procedure was followed for reactions at 2.5×10^{-4} M of $[1]^{2-}$ in CH_3CN with 1 equiv of DMAD (see main text) or with 10 equivalents of DMAD (Fig. S27).

Fitting of absorption traces.

The decay of intermediate **A** and the growth of $[2]^{2-}$ and $[3]^{2-}$ were fit using MATLAB R2018b software to deconvolute the electronic absorption spectra. Specifically, the isolated absorption spectrum of $[3]^{2-}$ was calculated by subtraction of the absorbance of a CH_3CN solution of pure $[2]^{2-}$ from the spectrum of the reaction mixture after complete conversion of $[1]^{2-}$ to $[2]^{2-}$ and $[3]^{2-}$ (Fig. S24). The absorption spectrum of intermediate **A** was calculated by subtraction of contributions from $[3]^{2-}$ (0.09 equiv at time 0 measured by 1H NMR spectroscopy) from the spectrum of the reaction mixture taken from the first time point (Fig. S28).

The absorption spectra (300–800 nm) were fit using non-linear least squares regression to calculate the concentrations of **A**, $[2]^{2-}$, and $[3]^{2-}$ over time (Fig. S29). The decay of **A** and the growth of $[2]^{2-}$ and $[3]^{2-}$ were then modeled using a second-order integrated rate law using the MATLAB CurveFitting toolbox.



Second-order Rate Law:

$$-\frac{d[A]}{dt} = 2 \frac{d[\mathbf{2}^{2-}]}{dt} = 2 \frac{d[\mathbf{3}^{2-}]}{dt} = k[A]^2 \quad (\text{S2})$$

Integrated Rate Laws:

$$[A]_t = \frac{1}{kt + \frac{1}{[A]_0}} \quad (\text{S3})$$

$$[\mathbf{2}^{2-}]_t = -\frac{1}{2[kt + \frac{1}{[A]_0 - [\mathbf{2}^{2-}]_0}]} + \frac{[A]_0}{2} \quad (\text{S4})$$

$$[\mathbf{3}^{2-}]_t = -\frac{1}{2[kt + \frac{1}{[A]_0 - [\mathbf{3}^{2-}]_0}]} + \frac{[A]_0}{2} \quad (\text{S5})$$

Best Fit Parameters:

$$k = 36.66 \text{ M}^{-1} \text{ s}^{-1}, [A]_0 = 2.39 \times 10^{-4} \text{ M}, [\mathbf{2}^{2-}]_0 = 0 \text{ M}, [\mathbf{3}^{2-}]_0 = 2.0 \times 10^{-5} \text{ M}$$

$$R^2 \text{ of } \mathbf{A}: \quad 0.99$$

$$R^2 \text{ of } [\mathbf{2}^{2-}]: \quad 0.9742$$

$$R^2 \text{ of } [\mathbf{3}^{2-}]: \quad 0.9181$$

The concentrations $[A]_t$ and of $[\mathbf{2}^{2-}]_t$ were also adjusted by constants of $8.17 \times 10^{-6} \text{ M}$ and $-9.8 \times 10^{-6} \text{ M}$, respectively. These discrepancies, along with the low R^2 values, likely arise from other side reactions and byproducts formed, some of which were also observed by ^1H NMR spectroscopy.

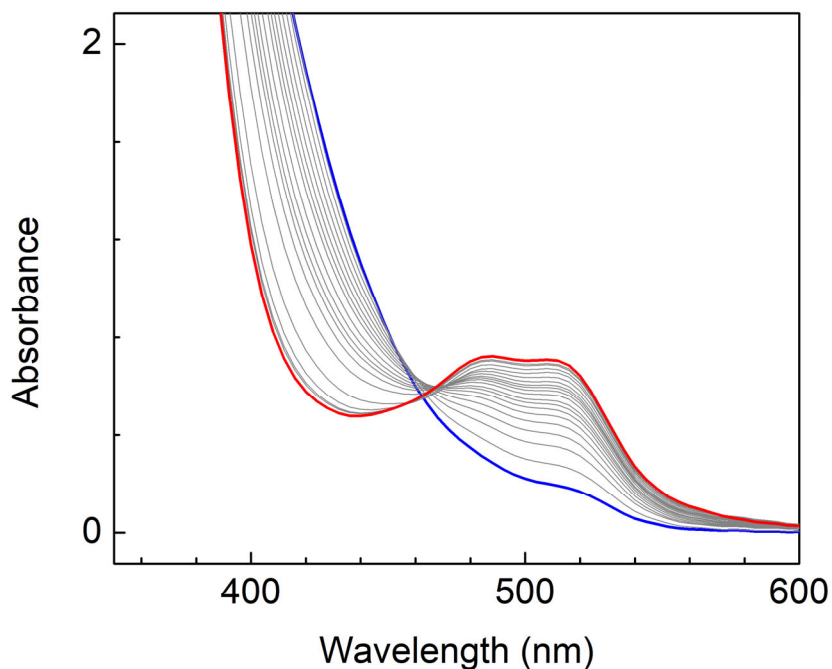


Figure S27. Electronic absorption spectra of a mixture of $[\text{Et}_4\text{N}]_2[\mathbf{1}]$ and DMAD (1 equiv) at 5.0×10^{-4} M in CH_3CN . The blue trace is the initial spectrum taken within 30 seconds of mixing. The red trace is the final spectrum taken of the mixture after several hours.

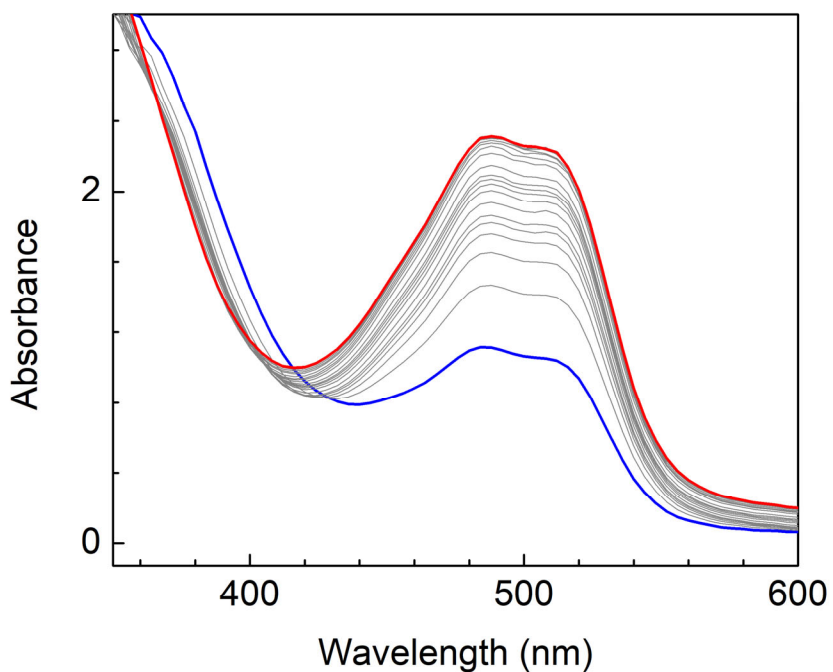


Figure S28. Electronic absorption spectra of a mixture of $[\text{Et}_4\text{N}]_2[\mathbf{1}]$ and DMAD (10 equiv) at 2.5×10^{-4} M in CH_3CN . The blue trace is the initial spectrum taken within 30 seconds of mixing. The red trace is the final spectrum taken of the mixture after several hours.

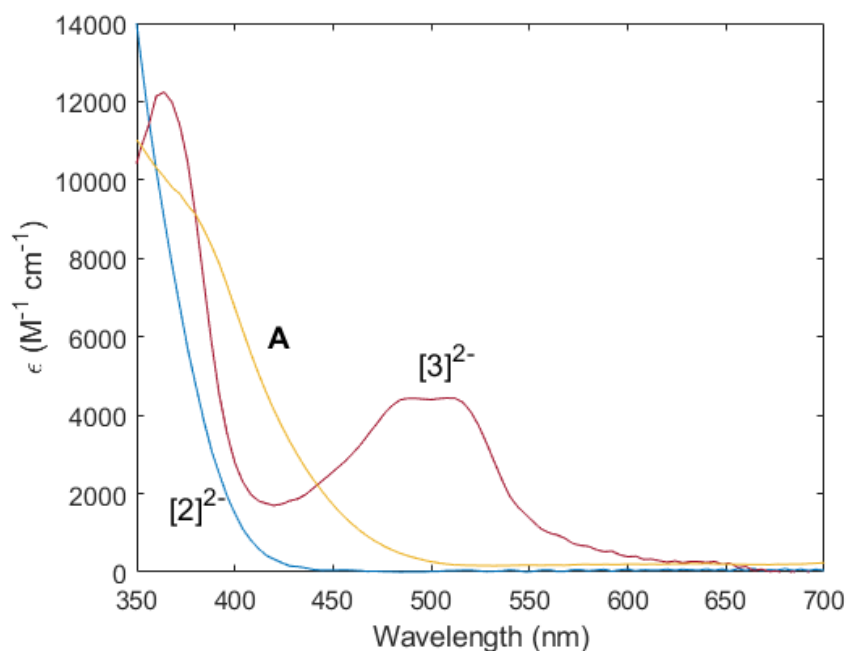


Figure S29. Electronic absorption spectra of A, $[2]^{2-}$, and $[3]^{2-}$ calculated as described.

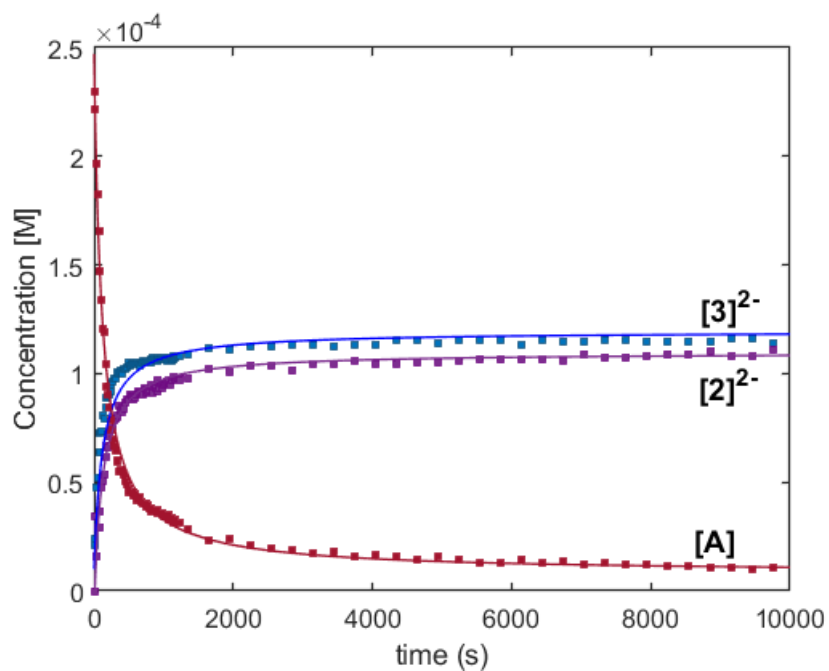


Figure S30. Concentrations of A (red), $[2]^{2-}$ (purple), and $[3]^{2-}$ (blue) plotted over time for a mixture of $[1]^{2-}$ (2.5×10^{-4} M, CH_3CN) and DMAD (1.1 equiv). Lines indicate fits to a second-order rate law.

Crystallographic Information

CCDC 1996091 and 1996092 contain the supplementary crystallographic data for this paper. These data can be obtained free of charge from The Cambridge Crystallographic Data Centre via www.ccdc.cam.ac.uk/data_request/cif.

Refinement Details for [Et₄N]₂[2]. Crystals were mounted on a MiTeGen loop using Paratone oil, then placed on the diffractometer under a cold nitrogen stream. An arbitrary sphere of data was collected on a light yellow block-like crystal, having approximate dimensions of 0.185 × 0.155 × 0.135 mm, on a Bruker APEX-II CCD diffractometer using a combination of ω- and φ-scans of 0.5°. Data were corrected for absorption and polarization effects and analyzed for space group determination.⁷ The structure was solved by dual-space methods and expanded routinely.⁸ The model was refined by full-matrix least-squares analysis of F² against all reflections.⁹ All non-hydrogen atoms were refined with anisotropic atomic displacement parameters. Unless otherwise noted, hydrogen atoms were included in calculated positions. Atomic displacement parameters for the hydrogens were tied to the equivalent isotropic displacement parameter of the atom to which they are bonded (U_{iso}(H) = 1.5U_{eq}(C) for methyl, 1.2U_{eq}(C) for all others).

Refinement Details for [Et₄N]₂[3]. Crystals were mounted on a MiTeGen loop using Paratone oil, then placed on the diffractometer under a cold nitrogen stream. An arbitrary sphere of data was collected on a red block-like crystal, having approximate dimensions of 0.23 × 0.213 × 0.134 mm, on a Bruker APEX-II CCD diffractometer using a combination of ω- and φ-scans of 0.5°. Data were corrected for absorption and polarization effects and analyzed for space group determination.⁷ The structure was solved by dual-space methods and expanded routinely.⁸ The model was refined by full-matrix least-squares analysis of F² against all reflections.⁹ All non-hydrogen atoms were refined with anisotropic atomic displacement parameters. Unless otherwise noted, hydrogen atoms were included in calculated positions. Atomic displacement parameters for the hydrogens were tied to the equivalent isotropic displacement parameter of the atom to which they are bonded (U_{iso}(H) = 1.5U_{eq}(C) for methyl, 1.2U_{eq}(C) for all others).

Table S1. Crystal and refinement data.

Compound	[Et ₄ N] ₂ [2]	[Et ₄ N] ₄ [3]
Empirical formula	C ₅₆ H ₆₅ N ₉ O ₄ S ₆ Zn	C ₂₈ H ₅₂ N ₂ O ₈ S ₄ Zn
Formula weight	1185.90	738.32
Temperature	120 K	120 K
Wavelength	0.71073 Å	0.71073 Å
Crystal system	Triclinic	Triclinic
Space group	P-1	P-1
Unit cell dimensions	$a = 12.7592(15)$ Å $b = 13.6618(17)$	$a = 8.8573(10)$ Å $b = 9.1035(10)$ Å

	Å	
	$c = 18.171(2) \text{ \AA}$	$c = 25.109(3) \text{ \AA}$
	$\alpha = 107.544(2)^\circ$	$\alpha = 80.268(2)^\circ$
	$\beta = 105.251(2)^\circ$	$\beta = 86.330(2)^\circ$
	$\gamma = 98.746(2)^\circ$	$\gamma = 61.6180(10)^\circ$
Volume	$2820.1(6) \text{ \AA}^3$	$1755.3(3) \text{ \AA}^3$
Z	2	2
Density (calculated)	1.397 g.cm^{-3}	1.397 g.cm^{-3}
Absorption coefficient (μ)	0.712 mm^{-1}	0.985 mm^{-1}
F(000)	1244	784
Crystal color, habit	light yellow, block	red, block
Crystal size	$0.185 \times 0.155 \times$ 0.135 mm^3	$0.23 \times 0.213 \times$ 0.134 mm^3
θ range for data collection	1.244 to 26.417°	0.823 to 28.364°
Index ranges	$-15 \leq h \leq 15, -17$ $\leq k \leq 17, -22 \leq l$ ≤ 22	$-11 \leq h \leq 11, -12$ $\leq k \leq 12, -33 \leq l$ ≤ 33
Reflections collected	56690	34171
Independent reflections	11508 [$R_{\text{int}} =$ 0.0540]	8760 [$R_{\text{int}} =$ 0.0152]
Completeness to θ $= 25.242^\circ$	100.0 %	100.0 %
Absorption correction	Semi-empirical from equivalents	Semi-empirical from equivalents
Max. and min. transmission	0.7454 and 0.6385	0.7457 and 0.7171
Refinement method	Full-matrix least-squares on F^2	Full-matrix least- squares on F^2
Data / restraints / parameters	11508 / 0 / 694	8760 / 0 / 400
Goodness-of-fit on F^2	1.033	1.024
Final R indices [$I > 2\sigma(I)$]	$R_1 = 0.0430,$ $wR_2 = 0.1102$	$R_1 = 0.0207, wR_2$ $= 0.0517$

R indices (all data)	R ₁ = 0.0598, wR ₂ = 0.1205	R ₁ = 0.0233, wR ₂ = 0.0531
Extinction coefficient	n/a	n/a
Largest diff. peak and hole	1.432 and -0.740 e ⁻ .Å ⁻³	0.416 and -0.173 e ⁻ .Å ⁻³

References

1. A. B. Pangborn, M. A. Giardello, R. H. Grubbs, R. K. Rosen and F. J. Timmers, *Organometallics*, 1996, **15**, 1518-1520.
2. M. Ballesteros and E. Y. Tsui, *Inorg. Chem.*, 2019, **58**, 10501-10507.
3. A. K. Verma, T. B. Rauchfuss and S. R. Wilson, *Inorg. Chem.*, 1995, **34**, 3072-3078.
4. S. Gracia, G. Arrachart, C. Marie, S. Chapron, M. Miguiditchian and S. Pellet-Rostaing, *Tetrahedron*, 2015, **71**, 5321-5336.
5. J. S. Bradshaw, G. E. Maas, J. D. Lamb, R. M. Izatt and J. J. Christensen, *J. Am. Chem. Soc.*, 1980, **102**, 467-474.
6. APEX-3, Bruker AXS. Madison, Wisconsin, USA, 2016.
7. L. Krause, R. Herbst-Irmer, G. M. Sheldrick and D. Stalke, *J. Appl. Cryst.*, 2015, **48**, 3-10.
8. G. M. Sheldrick, *Acta Crystallogr., Sect. A*, 2015, **71**, 3-8.
9. G. M. Sheldrick, *Acta Crystallogr., Sect. C*, 2015, **71**, 3-8.